Mg isotope composition in beech forest ecosystems and variations induced by liming: insights from four experimental sites in Northern France

Mélanie Court, Gregory van Der Heijden, Pascale Louvat, Emile Bolou-Bi, Guillaume Caro, Julien Bouchez, Benoit Pollier, Serge Didier, Claude Nys, Laurent Saint-andré, et al.

Mg isotope composition in beech forest ecosystems and variations induced by liming: insights from four experimental sites in Northern France

Mélanie Court[1], Gregory van der Heijden[1], Pascale Louvat[2], Emile Bolou-Bi[3], Guillaume Caro[4], Julien Bouchez[2], Benoit Pollier[1], Serge Didier[1], Claude Nys[1], Laurent Saint-André[1] and Arnaud Legout[1]*

[1]: INRAE, BEF, F-54000 Nancy, France

[2]: Institut de Physique du Globe de Paris, Equipe Géochimie des Enveloppes Externes (CNRS - UMR 7154), 1 Rue Jussieu, 75005 Paris, France

[3]: Université Felix-Houphouët Boigny d'Abidjan-Cocody, UFR des Sciences de la Terre et des Ressources Minières, BPV 34 Abidjan, Côte d'Ivoire

[4]: Centre de Recherches Pétrographiques et Géochimiques (CNRS - UPR 2300), 15 Rue Notre Dame des Pauvres, 54501 Vandoeuvre-les-Nancy, France

* Corresponding author: arnaud.legout@inrae.fr

Abstract

Many forest soils are acidic and have very low plant-available pools of magnesium. Past and present sylvicultural, nutritional and/or climatic pressures endured by forest ecosystems can result in net losses of nutrients and ecosystem function losses. Liming with a carbonate product is an alternative to counteract these degradations but the effects of liming on the biogeochemical cycling of nutrients over time and the dynamics of Mg released from liming products are still unclear. We studied the Mg isotopes composition in four paired-treatment experimental beech forest ecosystems in northern France. At the sites where dolomitic lime was applied, the variation in exchangeable and foliar δ^{26}Mg demonstrated the direct contribution of dolomite-derived Mg to the replenishment of topsoil exchangeable pools and to tree nutrition improvement: dolomite-derived Mg was incorporated into the biological cycling which allows its retention on the mid to long term in the soil-plant system. At the sites limed with calcium carbonate, the changes in exchangeable and foliar Mg contents and δ^{26}Mg observed on the long term suggest that the applied product contained a small amount of Mg and/or that Mg cycling changed after liming, to cope in particular with the low Mg availability. Lastly, our results highlight the high δ^{26}Mg of the organic layer (humus):

fractionation processes occurring within this layer (mineralization/ageing of organic matter, preferential retention of ^{26}Mg) could explain these singular signatures that could greatly influence the topsoil Mg exchangeable pools.

Keywords: forest ecosystem, liming, biogeochemical cycling, Mg isotopes, dolomite lime, calcium carbonate

1. Introduction

Magnesium is an essential and major nutrient in forest ecosystems (Marschner 1995) which plays an important role in plants (Bush 1995; Epstein 1956; Kirkby & Mengel 1976; Marschner 1995; Schulze et al. 2005) and soils by contributing to the pH buffer capacity, soil structure and biological activity (Wolters 1991). In forest soils, plant-available pools of magnesium are assumed to be stored as exchangeable cations adsorbed on the cation exchange complex. This exchangeable pool may change over time in relation to ecosystem inputs (atmospheric deposition and mineral weathering) and outputs (leaching and storage in tree biomass), particularly under the influence of external pressure. Indeed, decreasing atmospheric inputs (Likens et al. 1996) or the intensification of biomass harvesting and silvicultural practices (Achat et al. 2015; Pyttel et al. 2015; Ranger et al. 2011; Thiffault et al. 2015) may lead to forest soil fertility degradation, most particularly in low soil fertility forest ecosystems which are expected to be the most sensitive (Jonard et al. 2015; Van der Heijden et al. 2011). When the pressure endured is too intense, this degradation may lead to the progressive losses of nutrients and ecosystem functions, forest decline being the final stage of this process (Court et al. 2018).

To mitigate such issues, carbonate products (typically calcium carbonate or dolostone) may be applied (liming operation) in order to decrease soil acidity, maintain or restore forest soil fertility and improve tree nutrition (Court et al. 2018). Many studies of forest ecosystem liming operations have been carried out to assess the effects on organic matter decomposition (Baath et al. 1980; Geissen & Brümmer 1999; Marschner & Waldemar Wilczynski 1991; Smolander et al. 1996; Vuorenmaa et al. 2017), soil biological activity and community (Balland-Bolou-Bi & Poszwa 2012; Clivot et al. 2012; Lepleux et al. 2013; Moore 2014; Moore et al. 2013), topsoil fertility and tree nutrition or growth at short (Burke & Raynal 1998; Huettl 1989; Meiwes et al. 2002; Moore & Ouimet 2014; Wilmot et al. 1996) and long term time scales (Bakker 1998; Forey et al. 2015; Long et al. 2015; Moore et al. 2012).

However, because fewer studies have investigated these effects at the ecosystem scale (considering at the same time the mineral soil, the soil organic layer and the trees), the long-term dynamics and impacts of liming on the biogeochemical cycling of nutrients remains poorly understood.

Following liming operations using dolostone or calcium carbonate, the Mg concentrations in the soil are expected to increase on the short-term from i) the dissolution of the dolostone (Mg input) and/or ii) induced shifts of biogeochemical processes in the ecosystem (e.g. change in organic matter decomposition, etc.). However, conventional approaches based on measurements of nutrient contents in the ecosystem over time are not sufficient to i) distinguish precisely the native from the non-native (i.e. liming product) sources of Mg and ii) determine the proportion of the input of Mg from the liming that remains in the ecosystem over time.

The study of the natural variations of Mg stable isotope ratios coupled with conventional approaches have be proven to be a powerful tool to trace sources and processes in forest ecosystems (Uhlig et al. 2017). In particular, Mg isotope ratios allowed to specify the dynamics of Mg in soil/plant systems and the study of isotopic fractionations of Mg has made it possible to identify specific biological and/or physicochemical processes (Black et al. 2008; Bolou-Bi et al. 2010; Bolou-Bi et al. 2012; Opfergelt et al. 2014; Schmitt et al. 2012; Tipper et al. 2010). Despite Mg isotopic fractionation processes in the soil/plant systems and the small range of isotopic variations at the scale of the globe (-4.6 to 0.8‰, Fig. 1), Mg isotope ratios can, under certain conditions, be used to trace ecosystem sources (Bolou-Bi *et al.*, 2012). A sufficient difference of Mg isotopic composition between the liming product and the Mg pools in the forest ecosystem may allow for tracing the fate and distribution of the Mg originating from the dissolution of the liming product, as demonstrated by Bolou-Bi et al. (2016) on two paired forest catchments in the Vosges Mountains (one control and one limed).

In a previous study, Court et al (2018) studied with conventional approaches five permanent paired (limed and control) experimental beech (Fagus sylvatica L.) plots in Northern France to define and quantify the ecosystem response to liming. The objective of the present study was to investigate the variations of Mg stable isotopes in four of the five experimental sites studied by Court et al (2018) in order to i) better characterize the processes controlling the Mg cycle in forest ecosystems and ii) gain insight on the dynamics of Mg released from the liming product and the biogeochemical cycling changes induced by liming practices.

2. Material and Methods

2.1. Study sites

Four experimental liming sites in Northern France were selected for this study to cover a range of soil and climatic conditions: Potées, Humont, Darney and Fougères. The sites were described in detail in a previous study (Court et al. 2018) and only a summarized description is given here. The Fougères site is located in Brittany (oceanic climate), the Darney and Humont sites in the Vosges Mountains (semi-continental climate) and the Potées site in the Ardennes (semi-continental climate). Precipitation was evenly distributed throughout the year for all sites and average annual precipitation calculated over the 1995–2016 period was close to 1000 mm for all sites except Humont which was *ca* 1600 mm. Site elevation ranges from 185 m (Fougères) to 570 m (Humont). All sites are situated within state-owned forests and are managed following the local forest management plan. The stands are composed of pure European beech (*Fagus sylvatica* L.) and originated from the natural regeneration of the forest at all sites except Potées (plantation in 1986). Bedrock at each site is sandstone in the Vosges Mountains, shale in the Ardennes, and granodiorite in Brittany. The soils at the different sites classified as Dystric or Luvic Cambisols (WRB 2006) and are acidic and nutrient poor.

2.2. Liming experimental design

At each liming assay site, a similar experimental design was set up prior to the liming operation. Replicated plots were assigned for each treatment, depending on the sites: 2 $Ca/MgCO_3$ and 2 control plots at Potées and Humont; 1 $CaCO_3$ and 1 control plot at Darney and 4 $CaCO_3$ and 4 control plots at Fougères. Sampling subplots were then defined within each plot to avoid edge effects and all the measurements and samplings were done within these subplots. More details are available in Court et al (2018).

The liming products and the applied amounts were adapted at each site in relation to the soil physical and chemical properties and tree nutrient requirements. The granulometry of the applied liming products was < 2 mm and the products were manually applied (2–3 cross passages to homogenize the product application).

At Fougères and Darney, the liming operation consisted of a single application of commercial calcium carbonate ($CaCO_3$), applied in 1971 at Darney (1070 $kg.ha^{-1}$ Ca) and in 1973 at Fougères (1070 $kg.ha^{-1}$ Ca). At Humont, the liming operation consisted of a single application of dolomitic limestone applied in 1991 (541 $kg.ha^{-1}$ Ca; 228 $kg.ha^{-1}$ Mg). At

Potées, a commercial product (Resilvert®, MEAC) mainly composed of dolomitic limestone with P and K additives was applied in 1995 (543 kg.ha^{-1} Ca; 120 kg.ha^{-1} Mg).

2.3. Site monitoring: Sampling and elemental analysis

Samples were collected at different dates after the application of the liming product. Pre-treatment samples were only available at the Potées site. The sampled ecosystem compartment (organic layer, mineral soil and green leaves) and the corresponding sampling dates are detailed in Court et al (2018). The physical and chemical analysis of the different samples was performed directly after sampling.

2.3.1. Organic layer

The organic layer samples were collected using a 0.1 m² square frame. Three replicated samples were collected in each plot. The dry weight of the organic layer was measured for all replicates after oven-drying (35°C). Samples were milled and the three replicates were bulked together (one composite sample per plot) for further determinations. C and N contents were measured with a Thermo Quest NCS 2500. P, Mg, Ca and K contents were determined by ICP-AES after sample complete digestion in 50% nitric acid. Results represent the total amounts of nutrients in the organic layer.

2.3.2. Mineral soil

Mineral soil samples were collected at different depths with a soil auger (15 cm long helical auger for soil samples collected before 2000 and 15 cm long, 8 cm diameter cylindrical auger for samples collected after 2000). Three replicated soil profiles were sampled in each plot and a composite sample was generated for each sampled depth. Soil samples were air-dried and sieved (2 mm). Soil physical and chemical properties were analyzed by the INRA-ARRAS laboratory: humidity (NF ISO 11465), soil granulometry distribution (NF X 31-107), pH_{water} (soil water pH – 1:5 soil to water volume ratio) and pH_{KCl} (soil KCl pH – 1:5 soil to 0.1 mol.L^{-1} KCl reagent volume ratio) (NF ISO 10390), C and N content, cationic exchange capacity and exchangeable pools (Mg, Ca, K, Na, Al, H, and Mn) by cobaltihexamine (2.5 g of soil in a 50 mL of a 50 mmol$_c$.L^{-1} $Co(NH_3)_6^{3+}$ solution) (Standard method NF X 31-130) and soil total pools by hydrofluoric acid digestion (Mg, Ca, K, Na, Si, Al, Fe, Mn and P) (Standard method NF X 31-147).

2.3.3. Green tree leaves

Green leaves were sampled using a rifle at the end of the vegetation season (late august) from 3 branches in the top of the canopy collected from 3 dominant trees. A composite sample was generated for each plot. The nutrient content in green leaves was measured after oven-drying (65°C) and sample milling: C and N content was measured with a Thermo Quest NCS 2500. P, K, Ca, Mg, S, Mn content was determined by ICP-AES after sample digestion with 50% nitric acid. Results represent the total amounts of nutrients in foliage.

The majority of samples and liming products were then archived at the "Biogéochimie des Ecosystèmes Forestiers (INRAE)" laboratory.

2.4. Magnesium isotopic composition analysis

2.4.1. Sample preparation

The labware used during the treatment of the samples (*e.g.* pipette tips, tubes) was cleaned in an acid bath (2% HNO_3) before use for at least 24 hours and rinsed with ultrapure water (18.2 mΩ, PURELAB® Flex). The acids used were bidistilled (DST-1000 Savillex® distiller) to remove any impurities that may contaminate the samples. For sample acid digestion, Teflon® reactors were previously cleaned with concentrated acids in a scrubber (Analab®, ETC EVO II-ST). Sample processing and isotopic analysis were performed in a clean lab to avoid sample contamination.

The isotopic composition analysis were performed on a subset of the available samples. The selection of samples was based on the following criteria:

- Sites and years for which samples from the three studied compartments (soil, humus and tree foliage) were available.
- The most extreme years (beginning and end of monitoring) and, when possible, an intermediate year were favored.
- If the three compartments were not sampled within the same year, sampling dates for each compartment were selected as close as possible.

The selected samples were prepared differently for the isotopic analysis according to their type:

- For organic samples (green leaves and humus), 200 mg of sample was digested in 6 ml of 69% bidistilled HNO_3 and heated in a microwave oven (Anton Paar® Multiwave 3000). The solution was evaporated to dryness and 2 ml of 69% bidistilled HNO_3 were added.
- For total soil mineralization, the samples were digested in 1 ml of 40% HF for 24 hours at room temperature and then 4 ml of 69% bidistilled HNO_3 was added and samples were heated at 120°C for 48 h. The solution was evaporated to dryness and 2 ml of 37% bidistilled HCl were added and heated for 4 hours at 120°C. Then, the solution was again evaporated to dryness and 2 ml of 69% bidistilled HNO_3 were added.
- For soil exchangeable pool extractions, 4 g of sample were placed in a 50 mL Falcon tube with 40 ml of 1M ammonium acetate solution (Fractopur® NH_4OAc, Merck). The solution was continuously shaken during 1 hour and then centrifuged during 20 minutes at 3000 rpm. The supernatant was recovered and the extraction was repeated by adding 40 ml of 1M acetate ammonium solution, continuously shaking during 24h and centrifuging during 20 min at 3000 rpm. The exchangeable Mg extraction was done three times for each sample and the three replicates were bulked together in order to obtain a sufficient amount for isotope analysis, filtered (0.45 μm, nylon, Millipore®) and evaporated to dryness. The ammonium acetate was then digested by adding 5 mL of H_2O_2 (30% Suprapur®, Merck), evaporated to dryness and then taken up in 2 mL of 69% bi-distilled HNO_3.

2.4.2. Sample purification

Prior to Mg isotope composition measurements, each sample (soil and organic material digests and soil extracts) was purified according to a procedure adapted from Bolou-Bi et al. (2009). Purified Mg (~30μg) samples were obtained by ion-chromatography using a combination of AG®-MP-1M and AG®-50W-X12 resins:

- First the sample was eluted through an anion exchange resin (2mL AG®-MP-1M) using 7M HCl to elute cations with a high affinity for the anion exchange resin (e.g. Fe, Cu, Zn)

- Then the sample was sequentially purified through two cation exchange resin columns (2mL and then 1mL AG®-50W-X12). The samples were eluted with HNO_3 1M in the first column and with HCl 4M in the second.

The purified Mg solutions were evaporated to dryness.

2.4.3. Isotope ratio analysis

Mg stable isotope ratios ($^{26}Mg/^{24}Mg$ and $^{25}Mg/^{24}Mg$) were analysed with a multi-collector, inductively couple plasma mass spectrometer (MC-ICPMS) instrument (Neptune Plus, ThermoScientific), at the PARI analytical platform of the "Institut de Physique du Globe de Paris" (IPGP, Paris, France). The samples were diluted to 300 $\mu g.L^{-1}$ of Mg in 0.5M HNO_3 and introduced into the mass spectrometer through an Apex HF (ESI) equipped with a PFA concentric nebulizer (ESI, 50 $\mu l.min^{-1}$). The measurements were carried out with a medium resolution and by block of 25 cycles of 8s. Instrumental mass bias was monitored and corrected with the standard-sample bracketing technique using the DSM3 standard (Galy et al. 2003). Isotopic compositions are expressed in δ notation as the part per thousand (‰) deviation from the DSM3 standard (Equation 1):

(1) $$\delta^x Mg = \left(\frac{\frac{^x Mg}{^{24} Mg}(sample)}{\frac{^x Mg}{^{24} Mg}(DSM3)} - 1 \right) \times 10^3$$

where x is either mass 26 or 25.

Each sample was measured in triplicate (Std-Smpl-Std-Smpl-Std-Smpl-Std). Uncertainties from replicates are reported as two standard deviations (2SD).

For Potées (1995 and 2004) and Darney (1995), 0-5 cm and 5-15 cm soil layers were analyzed separately and the isotopic composition of the 0-15cm was calculated (supplementary material Fig. S1). For the other sites, the topsoil layers (0-5cm and 5-15cm) and the deep soil layers (30-45cm and 45-60cm) were bulked together prior to analysis (0-15cm and 30-60cm respectively) to reduce the number of samples to analyze.

The difference of Mg isotopic composition between control and limed plots is expressed in Δ notation (Equation 2):

(2) $$\Delta^{26} Mg_{Limed-Ctl} = \delta^{26} Mg_{Limed} - \delta^{26} Mg_{Control} \ (‰)$$

In the same way, the difference of Mg isotopic composition between two compartments A and B is expressed in Δ notation (Equation 3):

(3) $$\Delta^{26}Mg_{A-B} = \delta^{26}Mg_A - \delta^{26}Mg_B \text{ (‰)}$$

where A and B represent two different ecosystem compartments (e.g. Foliage (Fol), Organic layer (Org) or Exchangeable soil (Exch)).

2.4.4. Isotope ratio data validation

To assess measurement reproducibility, each sample was analysed several times in different sample sequences, *i.e.* at different dates. To assess measurement accuracy, standard solutions and reference materials were analysed in each sample sequence. The pure Mg 'Cambridge' standard was measured at the beginning and end of each sample sequence and was used as a reference to validate the results of the sample sequence. When the Cambridge standard measurements differed by more than 0.15‰ from the average value reported in the literature (-2.60‰), the δ^{26}Mg and δ^{25}Mg values of the samples measured during the same sequence were rejected. For the approved sample sequences, the Cambridge standard measurements were on average -2.61±0.09 ‰ (2SD, n=314). The reference materials that were analysed together with the samples were in good agreement with the accepted values: silicate rock reference material GA (Granite, δ^{26}Mg = -0.43±0.08 ‰, n=6), soil reference material Till1 (forest soil, δ^{26}Mg = -0.62±0.38 ‰, n=7), vegetation reference material BCR 281 (Rye Grass, δ^{26}Mg = -1.06±0.08 ‰, n=13) and sea water (BCR 403, δ^{26}Mg = -0.88±0.11 ‰, n=29), which validates both the Mg extraction protocol and the MC-ICP-MS analysis.

In addition, two indicators were used to check individual sample measurements:

1. To check the linearity of instrumental mass bias drift during a sequence, the δ^{26}Mg variation between two successive measurements of the DSM3 standard solution ("Dead Sea Magnesium") was estimated. Individual sample measurements were rejected if at least one of the two DSM3 bracketing showed a variation exceeding 0.15‰.
2. To check for mass-dependent fractionation (and thus for absence of isobaric interferences), each individual measurement was represented in a plot of Δ^{25}Mg' vs. δ^{26}Mg' (Young & Galy 2004), where (Equation 4):

(4) $$\delta^{X}Mg' = 1000 \times \log\left(\frac{\delta^{X}Mg + 1000}{1000}\right)$$

and

$$\Delta^{25}Mg' = \delta^{25}Mg' - 0.521 \times \delta^{26}Mg'$$

An individual measurement was rejected if, in this plot, the distance between the measurement and the kinetic (slope = 0.511) or equilibrium (slope = 0.521) theoretical mass fractionation line was greater than 0.01.

2.5. Modeling Mg isotopic variations

In order to investigate the reasons underlying the isotopic differences between the limed and control plots, a simple pool and flux model taking into account isotopic fractionation processes was developed (supplementary material Fig. S2). The numerical model simulates the annual change of the isotopic composition of the exchangeable pool of Mg in the 0-15 cm soil layer as a function of 1) the input fluxes of Mg to this layer (atmospheric, mineral weathering and organic layer sources) and their respective isotopic composition and 2) the isotopic fractionation processes that may occur through the output fluxes (root absorption, Mg leaching). In the limed plots, the model takes into account the input of Mg from the liming product and its isotopic composition and assumes that all lime-derived Mg is released within the first year.

The model was then used to test different possible hypotheses for the Darney and Potées sites that are listed in supplementary material Table S3. Depending on the hypotheses tested, the model was sequentially run for a range of input variables (e.g. tree uptake and leaching Mg flux, isotopic fractionation factors). For each set of input parameters, the model calculates either the possible values for the isotopic fractionation factors or the possible values for the input sources in order to reproduce the isotopic composition of the Mg exchangeable pool in both plots. This modelling approach could not be carried out for the Fougères and Humont sites because there were too few isotope data at these sites.

At the Potées site, where the pre-treatment data was available for the limed plot and for more pools, and at which flux and isotope data were available for both treatment plots, the model simulated the isotopic composition of the soil exchangeable pool of Mg in the lime plot over the 1995 to 2004 period following the measured changes in the exchangeable Mg pool of the 0-15cm soil layer.

At the Darney site, less data was available. In order to overcome the lack of data on the Mg fluxes, their isotopic composition, and the associated isotopic fractionation processes, the

316 model was run to simulate both the isotopic composition of the soil exchangeable Mg in the
317 control and limed plots over the 1971 to 1995 period by 1) assuming that the exchangeable
318 Mg pool in the control plot and its isotopic composition remained constant over the period
319 (steady state), 2) assuming that model parameters related to Mg isotopic fractionation were
320 the same for both plots, and finally 3) calculating the differences of Mg fluxes between plots
321 in order to respect the measured change in Mg exchangeable pool in the limed plot.
322
323 **3. Results**
324 **3.1. Comparison with previous published data on terrestrial ecosystems**
325 The δ^{26}Mg values measured in the control and limed plots at each of the four forest
326 ecosystems were within the previously reported range of δ^{26}Mg variation (Fig. 1) for bulk
327 soil, soil exchangeable pool (-0.9 to -0.3‰ for the control plots; -1.4 to -0.7‰ for the limed
328 plots), organic layer and tree foliage (-1.4 to -0.4‰ for the control plots; -1.8 to -0.9‰ for the
329 limed plots) (Table 1). The δ^{26}Mg values of bulk soils (-0.8 to -0.6‰) were only measured at
330 Potées and were close to the lowest values observed in terrestrial ecosystems. The range of
331 δ^{26}Mg for organic layer samples measured in this study (-0.7 to -0.3‰ for the control plots; -
332 0.7 to -0.0‰ for the limed plots) was narrower than that of soil exchangeable pools and leaves
333 were close to previously published values (-0.54 to -0.20‰). Unfortunately, not all the
334 applied liming products were archived and Mg isotope analyses was possible only for the
335 product applied at Potées (δ^{26}Mg = -1.60‰) and Humont (δ^{26}Mg = -1.56‰). This isotopic
336 composition was within the reported range of variation of dolomite (-2.2‰ to -1.1‰).
337
338 **3.2. Mg isotope compositions of green leaves, soils and organic layer in the control**
339 **plots**
340 In the control plots, differences between δ^{26}Mg values of different compartments were, on
341 average, noticeable between sites and may be ranked as follow (Fig. 2):
342 - Potées > Humont > Fougères and Darney for green leaves
343 - Humont > Darney > Potées and Fougères for soil exchangeable pools
344 - Darney > Humont and Potées > Fougères for organic layer
345 The foliar δ^{26}Mg was lower than that of the [0-15cm] exchangeable pool of the soil at all sites
346 and years, except at Potées in 1995 (Ctl pre-treatment plot, $\Delta^{26}Mg_{Fol\text{-}Exch}$ = 0.05‰; Ca/$MgCO_3$
347 pre-treatment plot, $\Delta^{26}Mg_{Fol\text{-}Exch}$ = 0.06‰) and 2004 ($\Delta^{26}Mg_{Fol\text{-}Exch}$ = 0.12‰) (Table 2).

348 The organic layer was enriched in ^{26}Mg isotope compared to the foliage at all sites and years,
349 except at Potées in 2004 ($\Delta^{26}Mg_{Fol\text{-}Org}$ = 0.08‰). At the four sites, the $\delta^{26}Mg$ of the organic
350 layer was slightly higher than the $\delta^{26}Mg$ of the [0-15cm] exchangeable pool of the soil, or
351 very close ($\Delta^{26}Mg_{Org\text{-}Exch}$ ranging from -0.11 to 0.18‰).
352
353 **3.3. Relationship between Mg concentration and Mg isotope composition in the**
354 **control plots**
355 In the control plots, differences in the foliar Mg concentrations were, on average, noticeable
356 between sites and may be ranked as follow: Fougères > Potées > Humont > Darney (Table 1).
357 Across the sampling sites, a positive relationship was observed between Mg concentrations
358 and $\delta^{26}Mg$ in the foliage in the control plots (Fig. 3), with Potées having the highest foliar Mg
359 concentration and $\delta^{26}Mg$ values, and Darney the lowest foliar Mg concentrations and $\delta^{26}Mg$
360 values. At Fougères, the intercept of the relation between foliar Mg concentrations and $\delta^{26}Mg$
361 was different (with higher foliar Mg concentrations compared to the other sites) but the slope
362 of the trend was very similar. The lowest Mg concentration and $\delta^{26}Mg$ in leaves at Fougères
363 were observed in 2005 whereas the highest were recorded in 2014.
364 In the control plots, the differences of $\delta^{26}Mg$ values between the organic layer and foliage
365 ($\Delta^{26}Mg_{Fol\text{-}Org}$) and between the [0-15cm] exchangeable pool of the soil and foliage ($\Delta^{26}Mg_{Fol\text{-}Exch}$) were larger when the foliar Mg concentration was low (Table 2 and supplementary
367 material Fig. S4). For the Mg isotope differences between compartments ($\Delta^{26}Mg_{Fol\text{-}Org}$ and
368 $\Delta^{26}Mg_{Fol\text{-}Exch}$), the sites were ranked as follow: Fougères and Potées < Humont < Darney. No
369 trend was observed between Mg concentrations and $\delta^{26}Mg$ or the Mg isotope differences
370 between compartments ($\Delta^{26}Mg$) for the organic pool and the [0-15cm] exchangeable pool of
371 the soil.
372
373 **3.4. Mg isotope variations between limed and control plots**
374 3.4.1. Foliage
375 For all sites foliage $\delta^{26}Mg$ of the limed plots were generally lower than those of the control
376 plots. The foliar $\delta^{26}Mg$ of the limed plots were ranked as follow: Potées > Fougères >
377 Humont > Darney (Fig. 2). Similar to the control plots, a high spatial and/or temporal
378 variability of the foliar $\delta^{26}Mg$ values were observed throughout the study period (Table 1). As
379 for the control plots, a positive relationship was observed between foliar Mg concentrations

and $\delta^{26}Mg$ values (Fig. 3). The foliar $\Delta^{26}Mg_{Limed-Ctl}$ was negative for all sites except Fougères in 2005 ($\Delta^{26}Mg_{Limed-Ctl}$ = 0.08 ‰) (Fig. 4). It increased gradually over time at Potées and Humont whereas it was stable over time at Fougères and Darney. As for the control plots, the $\delta^{26}Mg$ of foliage was lower than that of the [0-15cm] exchangeable pool of the soil in the limed plots at all sites (Fig. 2 and Table 2), except at Potées in 2004 ($\Delta^{26}Mg_{Fol-Exch}$ = 0.26‰). The trend between the $\Delta^{26}Mg_{Fol-Org}$ and foliar Mg concentration was not observed in the limed plots (Table 2 and supplementary material Fig. S4). As for the control plots, the $\Delta^{26}Mg_{Fol-Exch}$ was larger when the foliar Mg concentration was low in the limed plots, except at Potées in 2004. In terms of $\Delta^{26}Mg_{Fol-Exch}$, the sites were ranked as follow: Darney > Fougères > Potées and Humont.

3.4.2. Organic layer

In the limed plots, the $\delta^{26}Mg$ values of the organic layer were ranked as follow: Humont > Darney > Potées and Fougères (Fig. 2). The $\Delta^{26}Mg_{Limed-Ctl}$ of the organic layer was close to zero at Potées in 2004 and in 2016 ($\Delta^{26}Mg_{Limed-Ctl}$ = -0.06 ‰) and at Darney in 2016 ($\Delta^{26}Mg_{Limed-Ctl}$ = 0.01 ‰), slightly positive at Fougères in 2014 ($\Delta^{26}Mg_{Limed-Ctl}$ = 0.14 ‰), and widely positive at Humont in 2016 ($\Delta^{26}Mg_{Limed-Ctl}$ = 0.40 ‰) (Fig. 4). As for the control plots, the organic layer was enriched in ^{26}Mg compared to the foliage in limed plots but this enrichment in ^{26}Mg was larger in the limed plots than in the control plots (Fig. 2 and Table 2). No trend was observed between Mg concentration and $\delta^{26}Mg$ nor the Mg isotope differences between compartments ($\Delta^{26}Mg$) for the organic pool in limed plots.

3.4.3. Soils

In the limed plots, the $\delta^{26}Mg$ values of the [0-15cm] exchangeable pool of the soil were ranked as follow: Fougères and Darney > Potées > Humont (Fig. 2). Similar to the control plots, high spatial and/or temporal variability of the $\delta^{26}Mg$ was also observed for the [0-15cm] exchangeable pool of the soil at Potées throughout the study period (Table 1). The $\Delta^{26}Mg_{Limed-Ctl}$ of the [0-15cm] exchangeable pool of the soil were negative for all sites except Fougères ($\Delta^{26}Mg_{Limed-Ctl}$ = 0.07‰ in 1994) (Fig. 4). Humont had the largest $\Delta^{26}Mg_{Limed-Ctl}$ (-1.01‰, 25 years after liming). At Potées, the $\Delta^{26}Mg_{Limed-Ctl}$ was highest in 2004 (-0.68‰) and decreased to -0.34‰ in 2016. The $\Delta^{26}Mg_{Limed-Ctl}$ were smaller at Darney (mean $\Delta^{26}Mg_{Limed-Ctl}$ = -0.3‰), and did not vary over time. The $\delta^{26}Mg$ of the organic layer was higher than that of the [0-

15cm] exchangeable pool of the soil at all sites for the limed plots, and at Potées (2004) and Darney for the control plot (Fig. 2 and Table 2). Like the control plots, no trend was observed between Mg concentration and δ^{26}Mg or the Mg isotope differences between compartments (Δ^{26}Mg) and the [0-15cm] exchangeable pool of the soil in limed plots.

4. Discussion

4.1. Variations of the Mg isotope composition in forest ecosystems and possible controlling factors

4.1.1. Inter-site variability of weathering and atmospheric Mg input fluxes

The Mg isotopic composition of the 0-15cm exchangeable pool varied quite widely between the different studied sites. This variability could be partly due to the inter-site variability of the soil mineral weathering flux and isotopic composition. We do not have the δ^{26}Mg values of the bedrocks underlaying the four sites studied here. However, Darney and Humont are developed on Vosgian sandstone and Bolou-Bi et al. (2012) measured the δ^{26}Mg values of this bedrock (+0.13‰). In the same study, Bolou-Bi et al. (2012) also reported δ^{26}Mg values of the bulk soil that varied from -0.48‰ in the topsoil to +0.25‰ in the E horizon (30 cm depth) and +0.00‰ in the C horizon (110 cm depth). No data in this study or in the literature was available to characterize the isotopic signature of the loessic sedimentary deposits at Fougères and Potées but fine-grained sedimentary rocks are generally enriched in the light isotope ^{24}Mg compared to silicate rocks (Bolou-Bi et al. 2010). Under this assumption, the Mg mineral weathering flux in the 0-15cm soil layer would be more enriched in ^{24}Mg at Fougères and Potées compared to Darney and Humont which would contribute to explaining the observed inter-site δ^{26}Mg differences.

Though the Mg isotopic composition of the ocean and of the seawater-derived component of atmospheric inputs is relatively constant (between -0.7 and -0.9 ‰), the Mg isotopic composition of atmospheric inputs may vary from -1.05 to -0.51‰ (Bedel 2015; Bolou-Bi et al. 2012; Pogge von Strandmann et al. 2008; Tipper et al. 2010). No data is available to conclude on this issue, but Mg atmospheric inputs and their isotopic composition may also contribute to explain the observed inter-site δ^{26}Mg differences.

4.1.2. Relation between Mg plant-availability and Mg isotope variation

Similar to the soil, notable differences in foliar $\delta^{26}Mg$ values were observed between the control plots of the different studied sites. The range of variation of foliar $\delta^{26}Mg$ values was broader than that of the soil exchangeable pool and the foliage compartment was systematically enriched in ^{24}Mg compared to the soil exchangeable pool (except at Potées in 1995 and 2004). Previous studies on low-chemical fertility forest ecosystems have shown that Mg exchangeable pools in the top layers of the soil profile represent the main source of Mg for tree uptake (van der Heijden et al. 2015). Under this assumption, the $\delta^{26}Mg$ values of the [0-15cm] exchangeable pool alone could not explain the foliar $\delta^{26}Mg$ values. Therefore, it is most likely that isotopic fractionation processes occurring in the plant and/or between the soil and the foliage explain the $\Delta^{26}Mg_{Fol\text{-}Exch}$ observed in our data set, as suggested previously by several authors (Black et al. 2008; Bolou-Bi et al. 2010; Schmitt et al. 2012).

The $\Delta^{26}Mg_{Fol\text{-}Exch}$ varied between sites and the greatest values were observed at Humont and Darney where exchangeable Mg contents in the topsoil were amongst the lowest of the four studied sites. The $\Delta^{26}Mg_{Fol\text{-}Exch}$ was positively related to the foliage Mg concentration (supplementary material Fig. S4), which is commonly assumed to be a good indicator of the availability of nutrients in the ecosystem (Bonneau 1995). When the Mg availability in the soil decreases, the plant-internal recycling of Mg through the re-translocation processes occurring prior to litterfall contributes increasingly to sustaining Mg nutrition. Re translocation is known to fractionate Mg isotopes (Bedel 2015; Black et al. 2007; Bolou-Bi et al. 2016; Bolou-Bi et al. 2012; Kimmig et al. 2018; Kraj 2015; Matile 2000; Moynier & Fujii 2017). However, it is unlikely that foliar re-translocation dynamics explain the relation between $\Delta^{26}Mg_{Fol\text{-}Exch}$ and Mg concentration in foliage because it is ^{26}Mg that is preferentially transferred from the leaf to the younger tissues and/or to storage and reproductive organs of the tree (Bolou Bi et al, 2010). This suggests that low Mg availability in the soil may influence the isotopic fractionation processes that occur along the Mg uptake and allocation paths from the soil pools to the canopy.

4.1.3. Evidence of specific Mg isotope fractionation processes occurring in the organic layer and inheritance to the soil

Our results showed that the organic layer at each of the four sites was almost systematically the most ^{26}Mg-enriched compartment in the ecosystem. To our knowledge, few studies have investigated the Mg isotope composition of organic layers in forest ecosystems (Bolou Bi 2009; Mavromatis et al. 2014) and no mechanisms have yet been proposed to explain how the

organic layer becomes enriched in ^{26}Mg compared to the other compartments. In forest ecosystems, the Mg pool in the organic layer originates mostly from leaf litter inputs and atmospheric inputs that are retained on the cationic exchange capacity of the organic layer (van der Heijden et al. 2014). The $\delta^{26}Mg$ values of atmospheric inputs ranges from -1.05 to -0.51‰ (Bedel 2015; Bolou-Bi et al. 2012; Pogge von Strandmann et al. 2008; Tipper et al. 2010) and was lower than the $\delta^{26}Mg$ values of organic layers at all sites (except at Fougères). Furthermore, previous study in forest ecosystems highlight that leaf litter is slightly enriched in ^{24}Mg compared to green leaves due to re-translocation of the foliar Mg during the growing season (Bedel 2015; Black et al. 2007; Bolou-Bi et al. 2016; Bolou-Bi et al. 2012; Kimmig et al. 2018; Kraj 2015; Matile 2000; Moynier & Fujii 2017), which would imply that the $\delta^{26}Mg$ values of leaf litter at our four sites (not measured) was equal or below the measured foliar $\delta^{26}Mg$ values. It would thus not be possible to obtain the $\delta^{26}Mg$ values measured in the organic layer from the simple isotopic mixing of these two sources (*i.e.* leaf litter and atmospheric inputs).

Therefore, to explain the observed ^{26}Mg enrichment in the organic layer, we hypothesized that one or several processes fractionating Mg isotopes occur in this layer during the mineralization and ageing of organic matter (*i.e.* leading to the preferential release of ^{24}Mg, for example due the capacity of fungi to fractionate stable isotopes of magnesium when mobilizing base cations from an organic substrate; Fahad *et al.*, 2016; Pokharel *et al.*, 2017) and/or the transfer of atmospheric Mg inputs through the layer with a preferential adsorption/binding of ^{26}Mg on the cationic exchange capacity developed by the organic layer (Bolou-Bi et al, 2010; Chang, 2004). Under this hypothesis, these isotopic fractionation processes would most likely vary depending on the organic matter turnover rate and thus on the climatic and edaphic conditions.

Interestingly, the sites with the highest organic layer $\delta^{26}Mg$ values (Darney and Humont) also have the highest $\delta^{26}Mg$ values of [0-15cm] exchangeable pools. In forest ecosystems, the annual Mg flux released from the decomposition of the organic layer may represent a large input flux to the topsoil compared to atmospheric inputs and mineral weathering. The Mg isotopic composition of the topsoil Mg exchangeable pool is thus most probably greatly influenced by the Mg isotopic signature of the organic layer.

4.2. Effect of liming on Mg cycling and isotope composition

Calcium carbonate was applied at Fougères and Darney while dolomitic limestone ($Ca/MgCO_3$) was applied at Potées and Humont. We may consider that these products were probably completely dissolved in the first years following the application, due to rainfall and the high acidity of the organic and topsoil layers (pH<5). The isotopic composition of the dolomitic limestone was close to that measured by Bolou-Bi et al. (2016) (-1.75‰) and within the reported range of variation of dolomite 2.5‰ to -1‰ (Brenot et al. 2008; Jacobson et al. 2010). In contrast to dolomite lime, we were unable to perform analysis on the applied calcium carbonate, but the Mg content of such products is generally low ($MgCO_3$< 5%) with δ^{26}Mg values ranging from -5‰ to -4‰ (Galy et al. 2002). The δ^{26}Mg values of the [0-15cm] exchangeable pool and organic layer of the control plots (- 1‰ to -0.3‰) were always higher than that of applied products, while the range of variation for foliage δ^{26}Mg values sometimes overlapped it slightly (- 1.4‰ to -0.4‰), without compromising the tracing of Mg originating from the dissolution of the products.

4.2.1. Effect of dolomitic limestone ($Ca/MgCO_3$)

At the sites limed with dolomitic limestone, we observed lower δ^{26}Mg values and higher Mg concentrations in the [0-15cm] exchangeable pool and foliage in the limed plots compared to the control plots. The Mg isotopic approach provides here additional and useful information to distinguish the native from the non-native sources of Mg and our results strongly suggest that a significant part of foliar Mg originated from the dissolved dolomite and that the dolomite-derived Mg was quite rapidly incorporated in the biological cycle. The biological cycling of Mg then contributed to preserving the dolomitic Mg in the soil-plant system, and thus improving tree nutrition on the mid to the long-term. Bolou-Bi et al. (2016) showed similar patterns over a 10-years period after a dolomitic lime application in a limed forested catchment located in the Vosges Mountain. However, the efficiency of the biological cycle in maintaining the dolomite-derived Mg in the topsoil seemed to be limited at Potées compared to Humont: the δ^{26}Mg values of the topsoil exchangeable pools was significantly influenced by dolomite-derived Mg at Humont more than 15 years after liming and to a much lesser extent at Potées. Interestingly, the input-output budgets computed by Court et al. (2018) at Potées and the Mg concentrations in the different ecosystem compartments showed a small recovery of Mg released from the liming products (39% of Mg applied recovered in the ecosystem in 2004 and 12% in 2016), with a null recovery for soil in 2016. Court et al. (2018) hypothesized that a large fraction of the liming product was leached out of the ecosystem, but

541 the δ^{26}Mg values of the [0-15cm] exchangeable pool was still lower in the limed plot than in
542 the control plot 19 years after the product application. The modelling of the isotopic variations
543 (supplementary material Table S3) corroborates the hypothesis of elevated leaching losses
544 either by a leaching flush occurring in the first years after the application or by a leaching flux
545 associated with an isotopic fractionation (-0.2 to -0.6 ‰: preferential leaching of ^{24}Mg).
546
547 4.2.2. Effect of calcium carbonate ($CaCO_3$)
548 At Darney, the δ^{26}Mg values and the Mg content of the [0-15cm] exchangeable pool were
549 lower in the limed plot than in the control plot over the study period. Although these
550 differences could be due to spatial variability between the limed and control plots (the
551 available data was insufficient to fully dismiss such an effect), the lower δ^{26}Mg values in the
552 [0-15cm] exchangeable pool of the limed plot may be related to a shift in the biogeochemical
553 cycling of Mg occurring after the lime application. Several related hypotheses were tested
554 with the numerical modelling approach (supplementary material Table S3) and the results
555 show that the lower δ^{26}Mg values in the topsoil in the limed plot is most likely explained by a
556 small amount of Mg contained in the applied calcium carbonate, with an isotope signature of
557 δ^{26}Mg ~ 4.5‰. The lower foliar δ^{26}Mg values observed in the limed plot compared to the
558 control plot supports this hypothesis and may be partly associated to the δ^{26}Mg values
559 variations of the exchangeable pool at this site.
560 At Fougères, no difference in terms of exchangeable δ^{26}Mg values was observed between the
561 limed and the control plots, most likely because the calcium carbonate applied at the soil
562 surface did not contain any significant amount of Mg. It is unlikely that the change in foliar
563 δ^{26}Mg values observed in the limed plot at this site may be explained by an input of Mg
564 originating from the liming product. Court et al. (2018) showed that liming with calcium
565 carbonate induced on the long term (> 40 years) at Fougères and Darney a decrease in
566 exchangeable Mg content in the topsoil and foliar Mg concentrations. We may hypothesize
567 that a change in tree nutrition strategy occurred after liming (uptake distribution within the
568 soil profile) and/or, as discussed previously (see section 4.1.2), that the decreasing availability
569 of Mg in the soil changed the isotope fractionation processes in the plant, resulting in a
570 decrease of foliar δ^{26}Mg values at both sites (supplementary material Fig. S4).
571
572 4.2.3. Organic layer Mg isotope variations induced by liming

The only noticeable difference of $\delta^{26}Mg$ values between limed and control plots for the organic layer was observed at the Humont site, with larger $\delta^{26}Mg$ values in the limed plot 25 years after liming ($\Delta_{Limed-Ctrl}{}^{26}Mg$ = 0.39‰ in 2016). We previously hypothesized that isotope fractionation processes may occur within the organic layer (see section 4.1.3), leading to an enrichment of this layer in ^{26}Mg. The enhancement of the organic matter mineralization induced by liming (Court et al. 2018; Forey et al. 2015) may have resulted in an enrichment of the organic layer in ^{26}Mg (through the preferential release of ^{24}Mg). This hypothesis is supported by the strong decrease of the organic layer dry weight at Humont (strongest decrease among all four sites, Court et al. (2018)) in the limed plot (2.09 $kg.m^{-2}$) compared to the control plot (5.55 $kg.m^{-2}$) which suggests that liming strongly impacted the dynamics of organic matter decomposition at this site.

For the other sites, given the lower foliar $\delta^{26}Mg$ values and exchangeable $\delta^{26}Mg$ values (Potées and Darney) and the lower organic layer dry weight (Fougères and Darney) in the limed plot compared to the control plot, we may have expected to observe a difference in the $\delta^{26}Mg$ values of the organic layer between limed and control plots. The changes in biogeochemical cycling induced by liming (increase of the mineralization rate of organic matter and of soil pH, Mg retranslocation before leaf abscission…) could partly explain the stability of the organic layer $\delta^{26}Mg$ values in the limed plot at these sites over time.

5. Conclusion

Biological cycling has been shown to have a great impact on stable Mg isotope ratio variations in terrestrial ecosystems and it has been argued that the range of Mg isotopic variations related to biotic processes is wider than the range related to abiotic processes. The $\delta^{26}Mg$ data from the present study also suggests that observed Mg isotopic variations in forest ecosystems are strongly controlled/influenced by biotic processes along the biological cycle (plant uptake and plant internal cycling, litterfall and organic matter decomposition). Our results also highlight the high $\delta^{26}Mg$ values of the organic layer, most likely explained by Mg isotope fractionation processes occurring within this layer (mineralization/ageing of organic matter, preferential retention/binding of ^{26}Mg). The results of this study show that future research should focus on understanding Mg isotope dynamics and their controlling factors in two key components of the biogeochemical cycle of Mg: the uptake and transport of Mg from the roots to the foliage and the supply, the storage and the release of Mg in the organic layer.

At plots where dolomitic lime was applied, the Mg content in the soil exchangeable pool, leaves foliage and organic layer increased in the 10 to 15 years after liming and then decreased slowly. The results from this isotopic tracing approach concur with the temporal pattern of response to liming observed through conventional elemental approaches: dolomite-derived Mg contributed to increase foliar concentrations and plant-available pools in the topsoil during the 10 to 15 years after the liming which then gradually decreased. However, magnesium isotopic variations also enable to demonstrate the incorporation of dolomite-derived Mg in the biological cycling and its retention on the mid to long term in the soil-plant system (at least 15 to 25 years after liming). At the sites limed with calcium carbonate, the conventional approaches showed a decrease in exchangeable Mg content in the topsoil and foliar Mg concentrations on the long term (30 to 45 years after liming). In the same time, a decrease of exchangeable and foliar δ^{26}Mg values was observed in the limed plots, suggesting that the applied product contained a small amount of Mg and/or that Mg cycling changed after liming, to cope in particular with the low Mg availability through shifts in soil organic matter mineralisation rates or in tree nutrition strategy.

The results of this study also highlight that, because carbonate liming has multiple effects on soil processes, reservoirs and nutrient cycling, conventional approaches (based on measurements of the content of Mg and of other nutrients such as Ca in the ecosystem over time) are most often insufficient to identify the direct effects of liming on the Mg cycle (i.e. the release of Mg contained in the liming product) from the indirect effects (*i.e.* the release and/or displacement of native Mg induced by liming). The isotopic approach coupled with numerical modelling tools provides additional information on the fate of the Mg released by liming products in the ecosystem. Because the difference in Mg isotopic signature between carbonate rocks and Mg pools in forest ecosystems is most often sufficiently big, the Mg released from the liming product can be traced in the ecosystem and its contribution to the different pools of Mg in the ecosystem can be quantified.

6. Acknowledgments

We gratefully acknowledge the financial support received from the Office National des Forêts, the Région Lorraine, GIP ECOFOR and the LTSER Zone Atelier Bassin Moselle.

We thank the Institut de Physique du Globe de Paris, « Géochimie des Enveloppes Externes » team for its welcome. MC-ICP-MS isotope analyses presented in this work were enabled by

the IPGP multidisciplinary program PARI and by the Region Île-de-France SESAME Grant no. 12015908.

The UR-1138 INRAE – Biogéochimie des Ecosystèmes Forestiers is supported by a grant overseen by the French National Research Agency (ANR) as part of the "Investissement d'Avenir" program (ANR-11-LABX-0002-01, Lab of Excellence ARBRE)

References

Achat D, Deleuze C, Landmann G, Pousse N, Ranger J, Augusto L (2015) Quantifying consequences of removing harvesting residues on forest soils and tree growth–A meta-analysis. Forest Ecology and Management 348: 124-141

Baath E, Berg B, Lohm U, Lundgren B, Lundkvist H, Rosswall T, Soderstrom B, Wirén A (1980) Effects of experimental acidification and liming on soil organisms and decomposition in a Scots pine forest. Pedobiologia 20(2): 85-100

Bakker M (1998) Effet des amendements calciques sur les racines fines de chêne (Quercus petraea et rohur) : conséquences des changements dans la rhizosphère.

Balland-Bolou-Bi C, Poszwa A (2012) Effect of calco-magnesian amendment on the mineral weathering abilities of bacterial communities in acidic and silicate-rich soils. Soil Biology and Biochemistry 50: 108-117

Bedel L (2015) Approche isotopique pour tracer la dynamique des éléments dans deux écosystèmes forestiers du plateau lorrain développés sur des sols polycycliques. In.

Bizzarro M, Baker JA, Haack H, Lundgaard KL (2005) Rapid timescales for accretion and melting of differentiated planetesimals inferred from 26Al-26Mg chronometry. The Astrophysical Journal Letters 632(1): L41

Black JR, Epstein E, Rains WD, Yin QZ, Casey WH (2008) Magnesium-isotope Fractionation During Plant Growth. Environmental Science and Technology 42(21): 7831-7836

Black JR, Yin Q-z, Rustad JR, Casey WH (2007) Magnesium isotopic equilibrium in chlorophylls. Journal of the American Chemical Society 129(28): 8690-8691

Bolou-Bi BE, Dambrine E, Angeli N, Pollier B, Nys C, Guerold F, Legout A (2016) Magnesium Isotope Variations to Trace Liming Input to Terrestrial Ecosystems: A Case Study in the Vosges Mountains. Journal of Environmental Quality 45(1): 276-284

Bolou-Bi E, Poszwa A, Leyval C, Vigier N (2010) Experimental determination of magnesium isotope fractionation during higher plant growth. Geochimica et Cosmochimica Acta 74(9): 2523-2537

Bolou-Bi E, Vigier N, Brenot A, Poszwa A (2009) Magnesium Isotope Compositions of Natural Reference Materials. Geostand. Geoanal. Res. 33(1): 95-109

Bolou-Bi EB, Vigier N, Poszwa A, Boudot J-P, Dambrine E (2012) Effects of biogeochemical processes on magnesium isotope variations in a forested catchment in the Vosges Mountains (France). Geochimica et Cosmochimica Acta 87: 341-355

Bolou Bi E (2009) Etude du rôle de la végétation dans le cycle biogéochimique du magnésium: approche isotopique. Université Henri Poincaré, Nancy 286:

Bonneau M (1995) Fertilisation des forêts dans les Pays tempérés. ENGREF, Nancy. Francia:

Brenot A, Cloquet C, Vigier N, Carignan J, France-Lanord C (2008) Magnesium isotope systematics of the lithologically varied Moselle river basin, France. Geochimica et Cosmochimica Acta 72(20): 5070-5089

Burke MK, Raynal DJ (1998) Liming influences growth and nutrient balances in sugar maple (Acer saccharum) seedlings on an acidic forest soil. Environmental and Experimental Botany 39(2): 105-116

Bush DS (1995) Calcium regulation in plant cells and its role in signaling. Annual review of plant biology 46(1): 95-122

Clivot H, Pagnout C, Aran D, Devin S, Bauda P, Poupin P, Guérold F (2012) Changes in soil bacterial communities following liming of acidified forests. Applied Soil Ecology 59: 116-123

Court M, van der Heijden G, Didier S, Nys C, Richter C, Pousse N, Saint-André L, Legout A (2018) Long-term effects of forest liming on mineral soil, organic layer and foliage chemistry: Insights from multiple beech experimental sites in Northern France. Forest Ecology and Management 409: 872-889

De Villiers S, Dickson J, Ellam R (2005) The composition of the continental river weathering flux deduced from seawater Mg isotopes. Chemical Geology 216(1): 133-142

Epstein E (1956) Mineral nutrition of plants: mechanisms of uptake and transport. Annual Review of Plant

691 Physiology 7(1): 1-24
692 Fahad ZA, Bolou-Bi EB, Köhler SJ, Finlay RD, Mahmood S (2016) Fractionation and assimilation of Mg
693 isotopes by fungi is species dependent. Environmental microbiology reports 8(6): 956-965
694 Forey E, Trap J, Aubert M (2015) Liming impacts Fagus sylvatica leaf traits and litter decomposition 25 years
695 after amendment. Forest Ecology and Management 353: 67-76
696 Galy A, Bar-Matthews M, Halicz L, O'Nions RK (2002) Mg isotopic composition of carbonate: insight from
697 speleothem formation. Earth and Planetary Science Letters 201(1): 105-115
698 Galy A, Yoffe O, Janney PE, Williams RW, Cloquet C, Alard O, Halicz L, Wadhwa M, Hutcheon ID, Ramon E,
699 Carignan J (2003) Magnesium isotope heterogeneity of the isotopic standard SRM980 and new reference
700 materials for magnesium-isotope-ratio measurements. J. Anal. At. Spectrom. 18(11): 1352-1356
701 Geissen V, Brümmer GW (1999) Decomposition rates and feeding activities of soil fauna in deciduous forest
702 soils in relation to soil chemical parameters following liming and fertilization. Biology and Fertility of Soils
703 29(4): 335-342
704 Huettl RF (1989) Liming and fertilization as mitigation tools in declining forest ecosystems. Water, Air, and Soil
705 Pollution 44(1): 93-118
706 Jacobson AD, Zhang Z, Lundstrom C, Huang F (2010) Behavior of Mg isotopes during dedolomitization in the
707 Madison Aquifer, South Dakota. Earth and Planetary Science Letters 297(3-4): 446-452
708 Jonard M, Fürst A, Verstraeten A, Thimonier A, Timmermann V, Potočić N, Waldner P, Benham S, Hansen K,
709 Merilä P, Ponette Q, de la Cruz AC, Roskams P, Nicolas M, Croisé L, Ingerslev M, Matteucci G, Decinti B,
710 Bascietto M, Rautio P (2015) Tree mineral nutrition is deteriorating in Europe. Glob Change Biol 21(1): 418-
711 430
712 Kimmig SR, Holmden C, Bélanger N (2018) Biogeochemical cycling of Mg and its isotopes in a sugar maple
713 forest in Québec. Geochimica et Cosmochimica Acta:
714 Kirkby EA, Mengel K (1976) The role of magnesium in plant nutrition. Zeitschrift für Pflanzenernährung und
715 Bodenkunde 139(2): 209-222
716 Kraj W (2015) Chlorophyll degradation and the activity of chlorophyllase and Mg-dechelatase during leaf
717 senescence in Fagus sylvatica. Dendrobiology 74:
718 Lepleux C, Uroz S, Collignon C, Churin JL, Turpault MP, Frey-Klett P (2013) A short-term mineral amendment
719 impacts the mineral weathering bacterial communities in an acidic forest soil. Research in Microbiology
720 164(7): 729-739
721 Likens GE, Driscoll CT, Buso DC (1996) Long-term effects of acid rain: response and recovery of a forest
722 ecosystem. Science 272(5259): 244
723 Long RP, Bailey SW, Horsley SB, Hall TJ, Swistock BR, DeWalle DR (2015) Long-Term Effects of Forest
724 Liming on Soil, Soil Leachate, and Foliage Chemistry in Northern Pennsylvania. Soil Science Society of
725 America Journal 79(4): 1223-1236
726 Marschner B, Waldemar Wilczynski A (1991) The effect of liming on quantity and chemical composition of soil
727 organic matter in a pine forest in Berlin, Germany. Plant and Soil 137(2): 229-236
728 Marschner H (1995) Mineral nutrition of higher plants. In: Marschner H (ed) Mineral Nutrition of Higher Plants
729 (Second Edition). Academic Press, London. p v-vi
730 Matile P (2000) Biochemistry of Indian summer: physiology of autumnal leaf coloration. Experimental
731 gerontology 35(2): 145-158
732 Mavromatis V, Prokushkin AS, Pokrovsky OS, Viers J, Korets MA (2014) Magnesium isotopes in permafrost-
733 dominated Central Siberian larch forest watersheds. Geochimica et Cosmochimica Acta 147(Supplement C):
734 76-89
735 Meiwes KJ, Mindrup M, Khanna PK (2002) Retention of Ca and Mg in the forest floor of a spruce stand after
736 application of various liming materials. Forest Ecology and Management 159(1–2): 27-36
737 Moore JD (2014) Short-term effect of forest liming on eastern red-backed salamander (Plethodon cinereus).
738 Forest Ecology and Management 318: 270-273
739 Moore JD, Ouimet R (2014) Effects of two types of Ca fertilizer on sugar maple nutrition, vigor and growth after
740 7 years. Forest Ecology and Management 320: 1-5
741 Moore JD, Ouimet R, Bohlen PJ (2013) Effects of liming on survival and reproduction of two potentially
742 invasive earthworm species in a northern forest Podzol. Soil Biology & Biochemistry 64: 174-180
743 Moore JD, Ouimet R, Duchesne L (2012) Soil and sugar maple response 15 years after dolomitic lime
744 application. Forest Ecology and Management 281: 130-139
745 Moynier F, Fujii T (2017) Theoretical isotopic fractionation of magnesium between chlorophylls. Sci Rep 7(1):
746 6973
747 Opfergelt S, Burton KW, Georg RB, West AJ, Guicharnaud RA, Sigfusson B, Siebert C, Gislason SR, Halliday
748 AN (2014) Magnesium retention on the soil exchange complex controlling Mg isotope variations in soils, soil
749 solutions and vegetation in volcanic soils, Iceland. Geochimica et Cosmochimica Acta 125: 110-130
750 Pogge von Strandmann PAE, James RH, van Calsteren P, Gislason SR, Burton KW (2008) Lithium, magnesium

751 and uranium isotope behaviour in the estuarine environment of basaltic islands. Earth and Planetary Science
752 Letters 274(3-4): 462-471
753 Pokharel R, Gerrits R, Schuessler JA, Floor GH, Gorbushina AA, von Blanckenburg F (2017) Mg Isotope
754 Fractionation during Uptake by a Rock-Inhabiting, Model Microcolonial Fungus Knufia petricola at Acidic
755 and Neutral pH. Environ. Sci. Technol. 51(17): 9691-9699
756 Pyttel PL, Kohn M, Bauhus J (2015) Effects of different harvesting intensities on the macro nutrient pools in
757 aged oak coppice forests. Forest Ecology and Management 349: 94-105
758 Ranger J, Augusto L, BERTHELOT A, BOUCHON J, CACOT E, DAMBRINE E, GAVALAND A, LACLAU
759 J-P, LEGOUT A, NICOLAS M, NYS C, PONETTE Q, OTTORINI J-M, SAINT-ANDRE L (2011)
760 Sylviculture et protection des sols. Ecole nationale du génie rural, des eaux et des forêts, Nancy, FRANCE
761 Schmitt A-D, Vigier N, Lemarchand D, Millot R, Stille P, Chabaux F (2012) Processes controlling the stable
762 isotope compositions of Li, B, Mg and Ca in plants, soils and waters: A review. Comptes Rendus Geoscience
763 344(11): 704-722
764 Schulze E-D, Beck E, Müller-Hohenstein K (2005) Plant Ecology.
765 Smolander A, Kitunen V, Paavolainen L, Mälkönen E (1996) Decomposition of Norway spruce and Scots pine
766 needles: Effects of liming. Plant and Soil 179(1): 1-7
767 Teng F-Z, Wadhwa M, Helz RT (2007) Investigation of magnesium isotope fractionation during basalt
768 differentiation: Implications for a chondritic composition of the terrestrial mantle. Earth and Planetary
769 Science Letters 261(1–2): 84-92
770 Thiffault E, Bechard A, Pare D, Allen D (2015) Recovery rate of harvest residues for bioenergy in boreal and
771 temperate forests: A review. Wiley Interdiscip. Rev. Energy Environ. 4(5): 429-451
772 Tipper ET, Gaillardet J, Louvat P, Capmas F, White AF (2010) Mg isotope constraints on soil pore-fluid
773 chemistry: evidence from Santa Cruz, California. Geochimica et Cosmochimica Acta 74(14): 3883-3896
774 Uhlig D, Schuessler JA, Bouchez J, Dixon JL, von Blanckenburg F (2017) Quantifying nutrient uptake as driver
775 of rock weathering in forest ecosystems by magnesium stable isotopes. Biogeosciences 14(12): 3111-3128
776 van der Heijden G, Dambrine E, Pollier B, Zeller B, Ranger J, Legout A (2015) Mg and Ca uptake by roots in
777 relation to depth and allocation to aboveground tissues: results from an isotopic labeling study in a beech
778 forest on base-poor soil. Biogeochemistry 122(2-3): 375-393
779 Van der Heijden G, Legout A, Nicolas M, Ulrich E, Johnson DW, Dambrine E (2011) Long-term sustainability
780 of forest ecosystems on sandstone in the Vosges Mountains (France) facing atmospheric deposition and
781 silvicultural change. Forest Ecol Manag 261(3): 730-740
782 Vuorenmaa J, Augustaitis A, Beudert B, Clarke N, de Wit HA, Dirnböck T, Frey J, Forsius M, Indriksone I,
783 Kleemola S (2017) Long-term sulphate and inorganic nitrogen mass balance budgets in European ICP
784 Integrated Monitoring catchments (1990–2012). Ecological Indicators 76: 15-29
785 Wiechert U, Halliday AN (2007) Non-chondritic magnesium and the origins of the inner terrestrial planets. Earth
786 and Planetary Science Letters 256(3): 360-371
787 Wilmot TR, Ellsworth DS, Tyree MT (1996) Base cation fertilization and liming effects on nutrition and growth
788 of Vermont sugar maple stands. Forest Ecology and Management 84(1): 123-134
789 Wolters V (1991) Soil Invertebrates-Effects on Nutrient Turnover and Soil Structure-A Review. Journal of Plant
790 Nutrition and Soil Science 154(6): 389-402
791 WRB (2006) World reference base for soil resources 2006. World Soil Resources Reports No. 103(FAO, Rome):
792 Young ED, Galy A (2004) The isotope geochemistry and cosmochemistry of magnesium. In: Johnson CM,
793 Beard BL & Albarede F (eds) Geochemistry of Non-Traditional Stable Isotopes. Reviews in Mineralogy &
794 Geochemistry. Mineralogical Soc America, Washington. p 197-230
795
796

Figure captions

Fig.1. Range of $\delta^{26}Mg$ variations in compartments of terrestrial ecosystems. Literature data* are presented for atmospheric deposition (dark blue), vegetation (green), soils (red), waters (light blue) and rocks (brown); data of this study are presented in white (control plots) and black (limed plots).

**(Bedel 2015; Bizzarro et al. 2005; Bolou-Bi et al. 2016; Bolou-Bi et al. 2009; Bolou-Bi et al. 2012; Brenot et al. 2008; De Villiers et al. 2005; Kimmig et al. 2018; Opfergelt et al. 2014; Teng et al. 2007; Wiechert & Halliday 2007; Young & Galy 2004).*

Fig.2. $\delta^{26}Mg$ variations in the different ecosystem compartments of the control (blue) and limed (dark red) plots of the studied sites: Potées (a), Humont (b), Fougères (c) and Darney (d).

Fig.3. Relationship between $\delta^{26}Mg$ and Mg foliar concentration in the control (blue) and limed (red) plots of the four study sites: Regression lines are presented in dashed lines for control plots (blue), limed plots (red) and control + limed plots (black).

Fig.4. Differences in Mg concentration (empty markers) and $\delta^{26}Mg$ (filled markers) between limed and control plots ($\Delta_{Limed\text{-}Control}{}^{26}Mg$) as a function of time after liming for the different ecosystem compartments of the four sites: [0-15cm] exchangeable soils (a), organic layers (b) and green leaves (c).

820 **Fig.1**

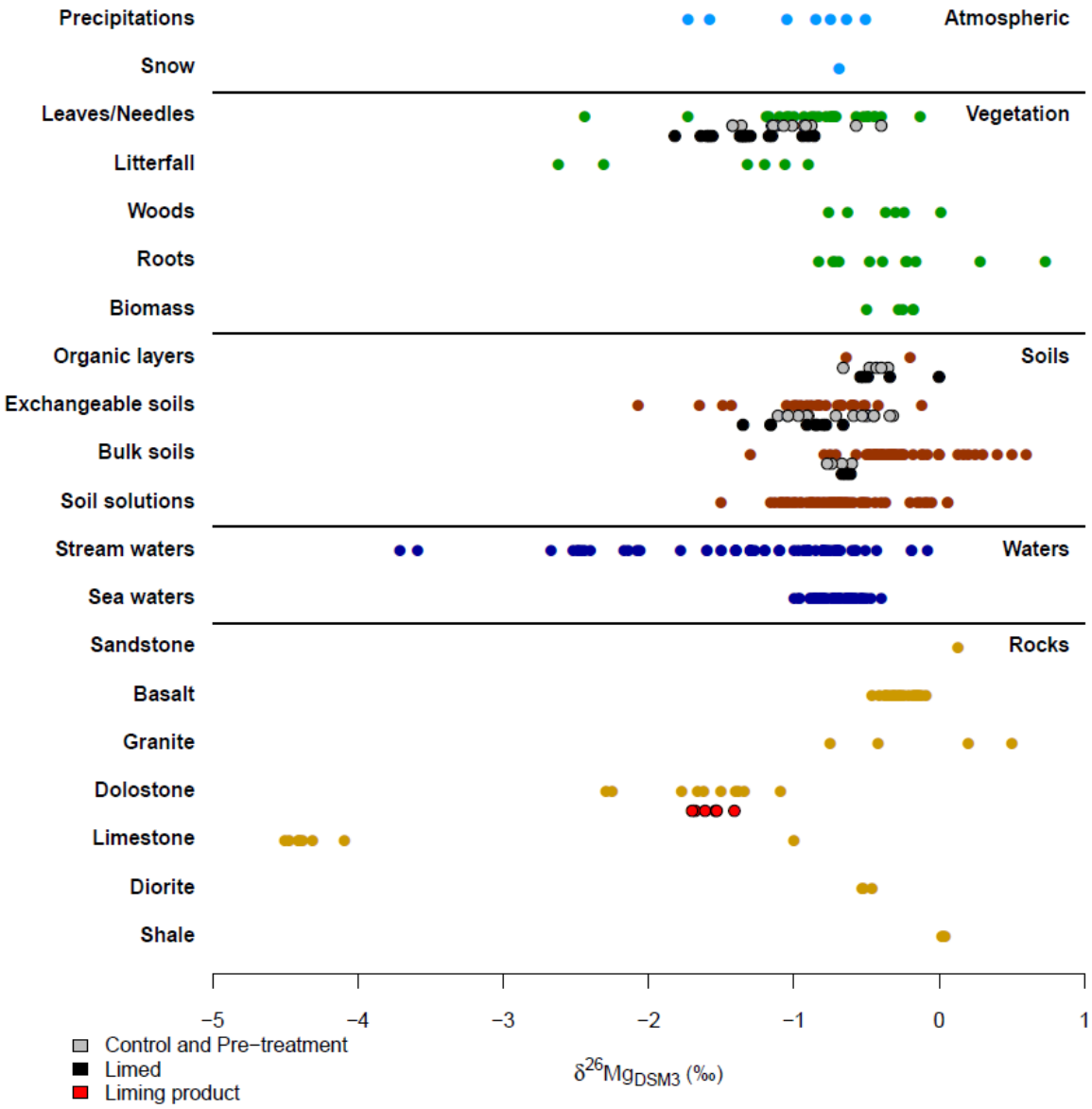
Precipitations
Snow
Leaves/Needles
Litterfall
Woods
Roots
Biomass
Organic layers
Exchangeable soils
Bulk soils
Soil solutions
Stream waters
Sea waters
Sandstone
Basalt
Granite
Dolostone
Limestone
Diorite
Shale
Atmospheric
Vegetation
Soils
Waters
Rocks
−5
−4
−3
−2
−1
0
1
Control and Pre−treatment
Limed
Liming product
δ26MgDSM3 (‰)

821

822 **Fig.2**

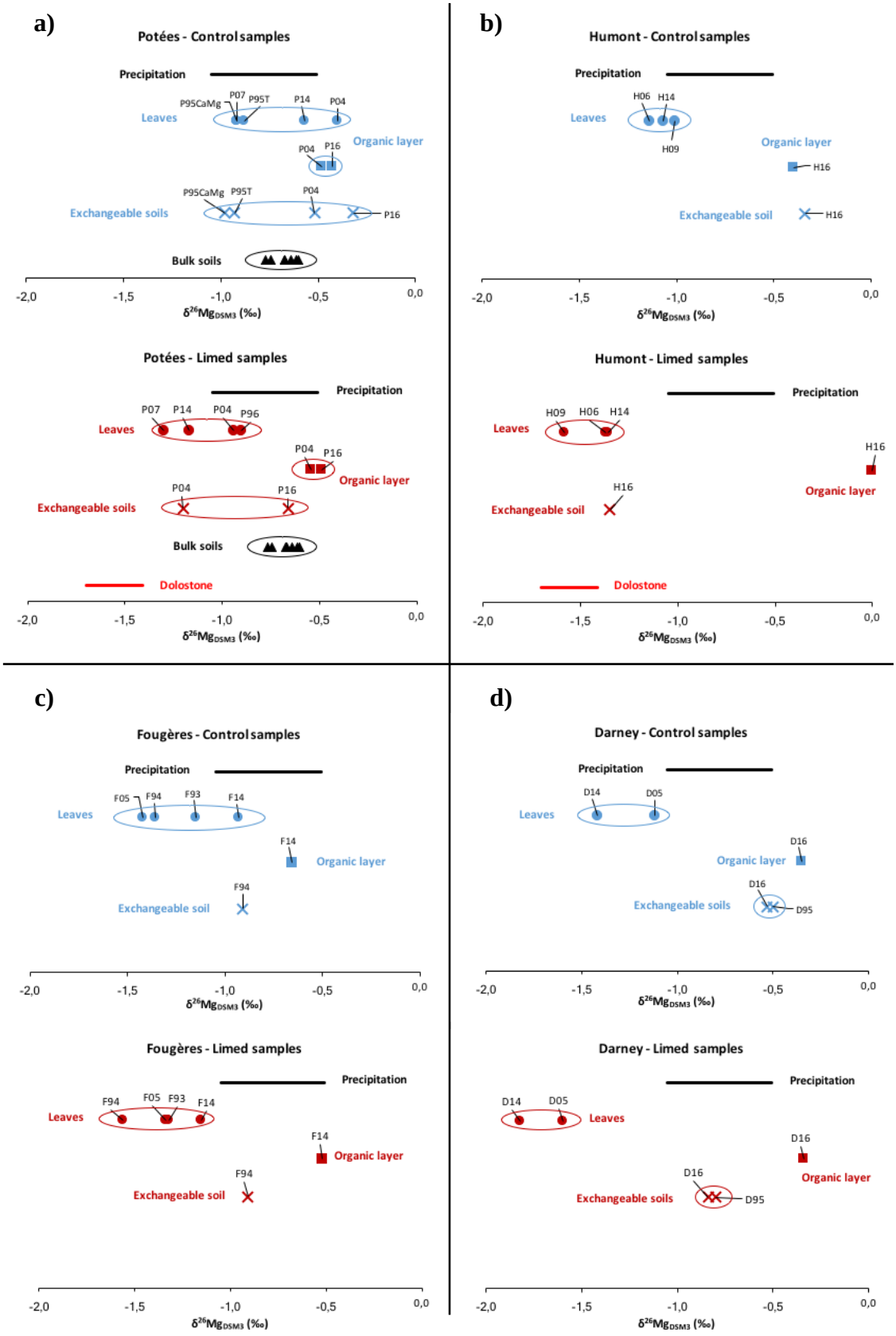
a)
Potées - Control samples
Precipitation
P95CaMg
P07
P95T
P14
P04
Leaves
Organic layer
P04
P16
P95CaMg
P95T
P04
Exchangeable soils
P16
Bulk soils
-2,0
-1,5
-1,0
-0,5
0,0
δ26MgDSM3 (‰)
Potées - Limed samples
Precipitation
P07
P14
P04
P96
Leaves
P04
P16
Organic layer
P04
P16
Exchangeable soils
Bulk soils
Dolostone
-2,0
-1,5
-1,0
-0,5
0,0
δ26MgDSM3 (‰)
b)
Humont - Control samples
Precipitation
H06
H14
Leaves
H09
Organic layer
H16
Exchangeable soil
H16
-2,0
-1,5
-1,0
-0,5
0,0
δ26MgDSM3 (‰)
Humont - Limed samples
Precipitation
H09
H06
H14
Leaves
H16
Organic layer
H16
Exchangeable soil
Dolostone
-2,0
-1,5
-1,0
-0,5
0,0
δ26MgDSM3 (‰)
c)
Fougères - Control samples
Precipitation
F05
F94
F93
F14
Leaves
F14
Organic layer
F94
Exchangeable soil
-2,0
-1,5
-1,0
-0,5
0,0
δ26MgDSM3 (‰)
Fougères - Limed samples
Precipitation
F94
F05
F93
F14
Leaves
F14
Organic layer
F94
Exchangeable soil
-2,0
-1,5
-1,0
-0,5
0,0
δ26MgDSM3 (‰)
d)
Darney - Control samples
Precipitation
D14
D05
Leaves
D16
Organic layer
D16
Exchangeable soils
D95
-2,0
-1,5
-1,0
-0,5
0,0
δ26MgDSM3 (‰)
Darney - Limed samples
Precipitation
D14
D05
Leaves
D16
Organic layer
D16
Exchangeable soils
D95
-2,0
-1,5
-1,0
-0,5
0,0
δ26MgDSM3 (‰)

826 **Fig.3**

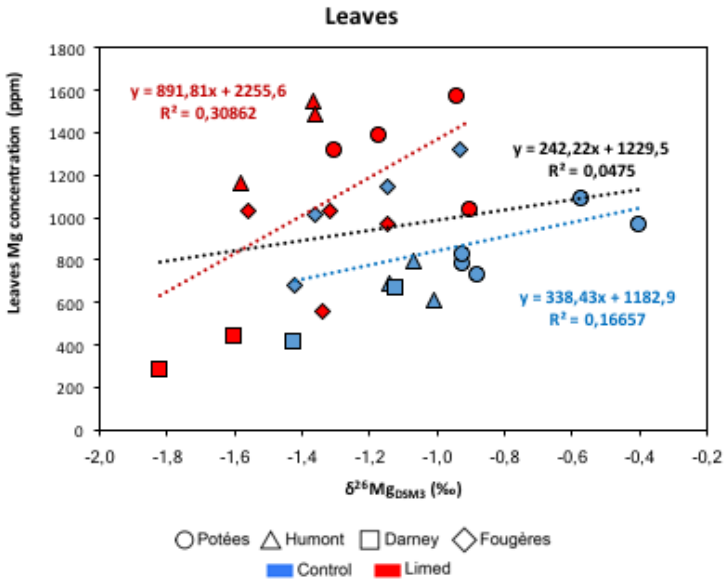

827

828

829 **Fig.4**

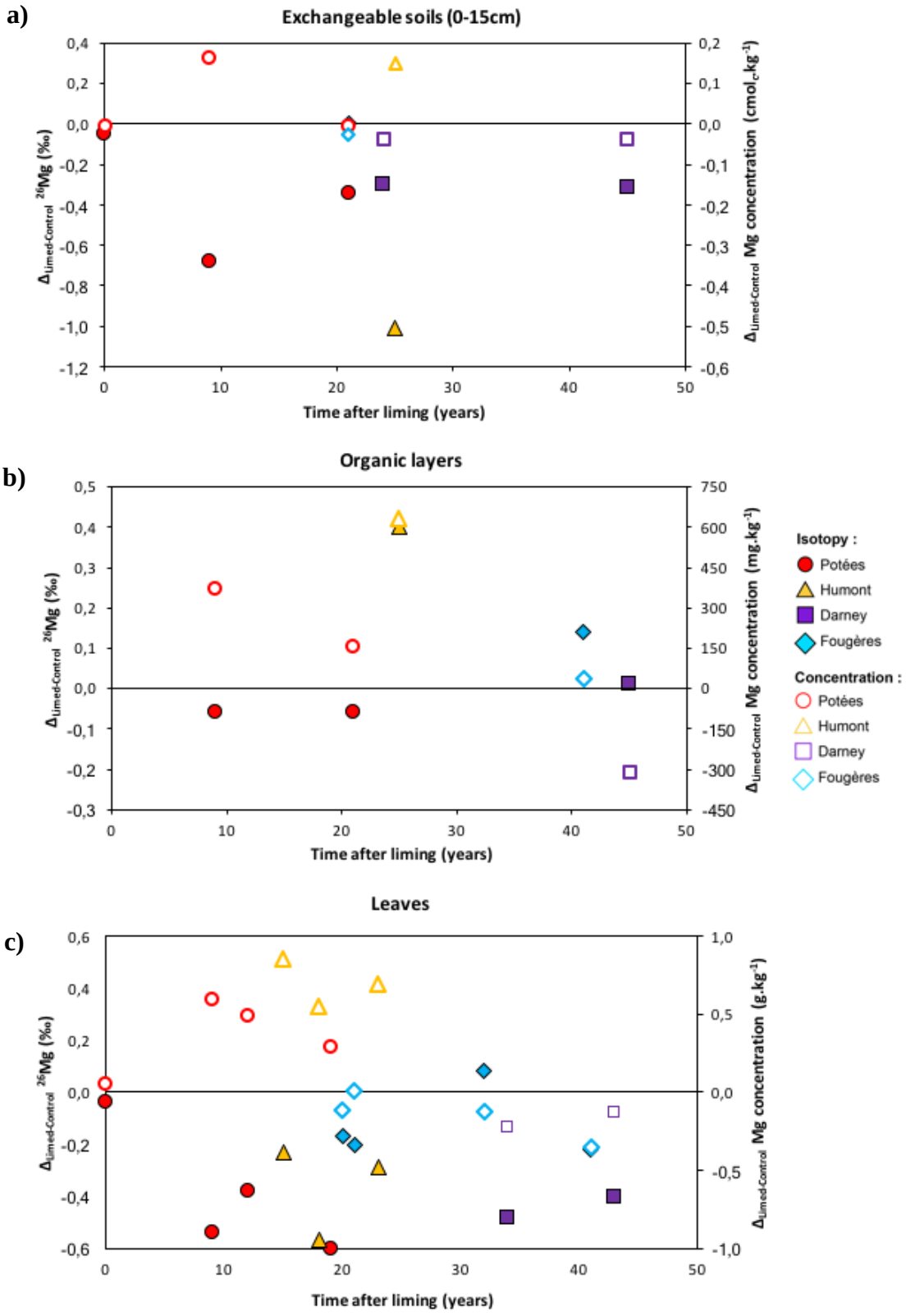
a)
Exchangeable soils (0-15cm)
Δ Limed-Control ²⁶Mg (‰)
Δ Limed-Control Mg concentration (cmol_c.kg⁻¹)
Time after liming (years)
b)
Organic layers
Δ Limed-Control ²⁶Mg (‰)
Δ Limed-Control Mg concentration (mg.kg⁻¹)
Time after liming (years)
Isotopy :
Potées
Humont
Darney
Fougères
Concentration :
Potées
Humont
Darney
Fougères
c)
Leaves
Δ Limed-Control ²⁶Mg (‰)
Δ Limed-Control Mg concentration (g.kg⁻¹)
Time after liming (years)

830

Table captions

Table 1. K, Ca and Mg concentrations and $\delta^{26}Mg$ of the leaves (a), organic layer (b) and [0-15cm] exchangeable soil pools (c) for each studied site. Slope, N and n values refer to the $\delta^{26}Mg$ analysis: N = number of sample sequences, n = number of validated replicates, n.a = not analysed, * = calculated values (see supplementary Fig. S1).

Table 2. Isotopic composition difference ($\Delta^{26}Mg$) between the different ecosystem compartments (leaves, organic layer and [0-15cm] exchangeable soils) for the control and limed plots of the studied sites.

Table 1 (a)

Sites	Treatments	Leaves										
		Years	K (ppm)	Ca (ppm)	Mg (ppm)	$\delta^{26}Mg_{DSM3}$ (‰)		$\delta^{25}Mg_{DSM3}$ (‰)		Slope	N	n
Potées	Control	1995	6273	4378	728	-0.88	0.13	-0.45	0.06	0.509	4	11
		1996	6482	4490	852	*n.a.*	*n.a.*	*n.a.*	*n.a.*	*n.a.*	*n.a.*	*n.a.*
		2004	8001	3523	966	-0.40	0.11	-0.20	0.05	0.508	4	9
		2007	6705	4832	820	-0.92	0.13	-0.46	0.06	0.504	2	5
		2014	5437	4646	1083	-0.57	0.16	-0.29	0.09	0.511	4	9
	Pre-treatment	1995	6218	4910	782	-0.92	0.04	-0.46	0.02	0.499	3	7
	$Ca/MgCO_3$	1996	5978	5996	1033	-0.90	0.07	-0.45	0.04	0.501	3	8
		2004	7943	5541	1569	-0.94	0.12	-0.48	0.06	0.511	6	15
		2007	7894	7453	1310	-1.30	0.14	-0.67	0.05	0.517	3	7
		2014	7398	7986	1380	-1.17	0.04	-0.60	0.02	0.515	3	7
Humont	Control	2006	8165	1834	695	-1.14	0.04	-0.59	0.05	0.514	3	9
		2009	10366	1622	612	-1.01	0.06	-0.52	0.03	0.519	2	5
		2014	8337	2115	792	-1.07	0.06	-0.55	0.03	0.514	2	4
	$Ca/MgCO_3$	2006	5728	5973	1551	-1.37	0.05	-0.72	0.04	0.518	2	6
		2009	9084	6170	1162	-1.58	0.05	-0.82	0.03	0.517	3	6
		2014	7316	5371	1489	-1.36	0.06	-0.70	0.02	0.513	2	5
Fougères	Control	1993	8627	3315	1147	-1.15	0.09	-0.59	0.04	0.514	4	11
		1994	8537	3826	1018	-1.36	0.07	-0.69	0.04	0.513	3	9
		2005	8796	2404	683	-1.42	0.10	-0.73	0.05	0.513	2	6
		2014	7025	4930	1322	-0.93	0.18	-0.47	0.08	0.509	3	8
	$CaCO_3$	1993	7519	6980	1032	-1.32	0.03	-0.68	0.02	0.517	3	9
		1994	8342	7348	1030	-1.56	0.09	-0.80	0.05	0.515	3	9
		2005	6348	6271	557	-1.34	0.07	-0.68	0.04	0.512	2	5
		2014	7254	7023	973	-1.15	0.05	-0.60	0.02	0.515	2	4
Darney	Control	1994	8850	3500	600	*n.a.*	*n.a.*	*n.a.*	*n.a.*	*n.a.*	*n.a.*	*n.a.*
		2005	9789	4589	661	-1.12	0.10	-0.57	0.06	0.512	3	8
		2014	11044	3074	410	-1.42	0.09	-0.72	0.05	0.504	2	6
	$CaCO_3$	1994	8900	7500	300	*n.a.*	*n.a.*	*n.a.*	*n.a.*	*n.a.*	*n.a.*	*n.a.*
		2005	10375	7067	433	-1.60	0.09	-0.80	0.05	0.508	2	6
		2014	10295	4867	277	-1.82	0.06	-0.93	0.04	0.511	2	6
Coat-an-Hay	Control	1995	7243	4100	914	*n.a.*	*n.a.*	*n.a.*	*n.a.*	*n.a.*	*n.a.*	*n.a.*
		2014	6837	4610	1278	*n.a.*	*n.a.*	*n.a.*	*n.a.*	*n.a.*	*n.a.*	*n.a.*
	$Ca/MgCO_3$	1995	6428	4192	1052	*n.a.*	*n.a.*	*n.a.*	*n.a.*	*n.a.*	*n.a.*	*n.a.*
		2014	8238	5550	1481	*n.a.*	*n.a.*	*n.a.*	*n.a.*	*n.a.*	*n.a.*	*n.a.*

Table 1 (b)

Sites	Treatments	Organic layer										
		Years	K (ppm)	Ca (ppm)	Mg (ppm)	$\delta^{26}Mg_{DSM3}$ (‰)		$\delta^{25}Mg_{DSM3}$ (‰)		Slope	N	n
Potées	Control	1995	4035	2861	1649	*n.a.*	*n.a.*	*n.a.*	*n.a.*	*n.a.*	*n.a.*	*n.a.*
		2004	2216	5088	732	-0.48	0.08	-0.25	0.03	0.517	2	5
		2007	2646	6112	910	*n.a.*	*n.a.*	*n.a.*	*n.a.*	*n.a.*	*n.a.*	*n.a.*
		2016	1689	7630	1031	-0.43	0.01	-0.22	0.01	0.509	1	2
	Pre-treatment	1995	3179	3737	1483	*n.a.*	*n.a.*	*n.a.*	*n.a.*	*n.a.*	*n.a.*	*n.a.*
	$Ca/MgCO_3$	2004	2022	7815	1103	-0.54	0.09	-0.28	0.05	0.518	5	10
		2007	2880	9027	1264	*n.a.*	*n.a.*	*n.a.*	*n.a.*	*n.a.*	*n.a.*	*n.a.*
		2016	1920	10023	1188	-0.66	0.11	-0.34	0.05	0.510	2	5
Humont	Control	2016	2104	3802	1065	-0.40	0.02	-0.20	0.01	0.502	3	8
	$Ca/MgCO_3$	2016	3264	4512	1699	0.00	0.13	0.01	0.06	0.893	3	9
Fougères	Control	1994	1242	4291	1058	*n.a.*	*n.a.*	*n.a.*	*n.a.*	*n.a.*	*n.a.*	*n.a.*
		2014	2441	5325	1422	-0.66	0.11	-0.34	0.05	0.510	2	5
	$CaCO_3$	1994	1368	8211	933	*n.a.*	*n.a.*	*n.a.*	*n.a.*	*n.a.*	*n.a.*	*n.a.*
		2014	1970	8973	1462	-0.52	0.13	-0.28	0.06	0.538	2	4
Darney	Control	2016	3356	4613	944	-0.35	0.12	-0.19	0.04	0.521	3	6
	$CaCO_3$	2016	1790	4049	636	-0.34	0.14	-0.17	0.08	0.517	4	8
Coat-an-Hay	Control	2014	1583	7632	2042	*n.a.*	*n.a.*	*n.a.*	*n.a.*	*n.a.*	*n.a.*	*n.a.*
	$Ca/MgCO_3$	2014	1481	10156	2142	*n.a.*	*n.a.*	*n.a.*	*n.a.*	*n.a.*	*n.a.*	*n.a.*

Table 1 (c)

Sites	Treatments	Exchangeable soils (0-15cm)										
		Years	K (ppm)	Ca (ppm)	Mg (ppm)	$\delta^{26}Mg_{DSM3}$ (‰)		$\delta^{25}Mg_{DSM3}$ (‰)		Slope	N	n
Potées	Control	1995	100	57	20	-0,93	0,05	-0,48	0,03	0,516	2+2*	6+5*
		2004	66	30	10	-0,52	0,01	-0,27	0,01	0,519	1+1*	2+3*
		2007	71	88	21	*n.a.*	*n.a.*	*n.a.*	*n.a.*	*n.a.*	*n.a.*	*n.a.*
		2016	53	39	12	-0,32	0,03	-0,16	0,02	0,513	2	5
	Pre-treatment	1995	99	59	19	-0,98	0,03	-0,50	0,02	0,510	1+2*	2+3*
		2004	64	210	30	-1,20	0,09	-0,62	0,05	0,517	3+2*	4+6*
	$Ca/MgCO_3$	2007	109	557	59	*n.a.*	*n.a.*	*n.a.*	*n.a.*	*n.a.*	*n.a.*	*n.a.*
		2016	43	62	11	-0,66	0,00	-0,34	0,00	0,515	3	3
Humont	Control	2007	118	29	23	*n.a.*	*n.a.*	*n.a.*	*n.a.*	*n.a.*	*n.a.*	*n.a.*
		2016	87	18	16	-0,34	0,11	-0,18	0,07	0,540	4	10
	$Ca/MgCO_3$	2007	119	426	73	*n.a.*	*n.a.*	*n.a.*	*n.a.*	*n.a.*	*n.a.*	*n.a.*
		2016	83	130	34	-1,35	0,04	-0,68	0,03	0,510	2	5
Fougères	Control	1994	103	75	37	-0,91	0,10	-0,47	0,06	0,511	3	8
		2014	72	75	34	*n.a.*	*n.a.*	*n.a.*	*n.a.*	*n.a.*	*n.a.*	*n.a.*
	$CaCO_3$	1994	88	278	33	-0,91	0,01	-0,48	0,00	0,528	2	4
		2014	34	24	13	*n.a.*	*n.a.*	*n.a.*	*n.a.*	*n.a.*	*n.a.*	*n.a.*
Darney	Control	1995	103	32	17	-0,50	0,05	-0,26	0,02	0,520	2+2*	8+3*
		2016	78	20	12	-0,53	0,04	-0,27	0,04	0,506	3	6
	$CaCO_3$	1995	104	92	12	-0,80	0,07	-0,41	0,04	0,512	1+1*	3+4*
		2016	65	26	8	-0,84	0,02	-0,44	0,01	0,521	2	4
Coat-an-Hay	Control	1995	92	76	40	*n.a.*	*n.a.*	*n.a.*	*n.a.*	*n.a.*	*n.a.*	*n.a.*
		2014	59	50	17	*n.a.*	*n.a.*	*n.a.*	*n.a.*	*n.a.*	*n.a.*	*n.a.*
	$Ca/MgCO_3$	1995	81	61	28	*n.a.*	*n.a.*	*n.a.*	*n.a.*	*n.a.*	*n.a.*	*n.a.*
		2014	54	153	35	*n.a.*	*n.a.*	*n.a.*	*n.a.*	*n.a.*	*n.a.*	*n.a.*

847 **Table 2**

Compartments	Sites	Treatment	Years	$\Delta_{compartments}{}^{26}Mg$ (‰)	$\Delta_{compartments}{}^{25}Mg$ (‰)
Leaves - Organic layer ($\Delta^{26}Mg_{Fol-Org}$)	**Potées**	Control	2004	0.08	0.05
			2014	-0.14	-0.07
		$Ca/MgCO_3$	2004	-0.40	-0.20
			2014	-0.68	-0.34
	Humont	Control	2014	-0.67	-0.35
		$Ca/MgCO_3$	2014	-1.36	-0.71
	Fougères	Control	2014	-0.27	-0.13
		$CaCO_3$	2014	-0.63	-0.32
	Darney	Control	2014	-1.07	-0.53
		$CaCO_3$	2014	-1.48	-0.76
Leaves - Exchangeable soil (0-15cm) ($\Delta^{26}Mg_{Fol-Exch}$)	**Potées**	Control	1995	0.05	0.03
			2004	0.12	0.07
			2016	-0.25	-0.13
		Pre-treatment	1995	0.06	0.04
		$Ca/MgCO_3$	2004	0.26	0.14
			2016	-0.51	-0.26
	Humont	Control	2016	-0.73	-0.37
		$Ca/MgCO_3$	2016	-0.01	-0.02
	Fougères	Control	1994	-0.45	-0.22
		$CaCO_3$	1994	-0.65	-0.32
	Darney	Control	2016	-0.89	-0.45
		$CaCO_3$	2016	-0.98	-0.49
Organic layer - Exchangeable soil (0-15cm) ($\Delta^{26}Mg_{Org-Exch}$)	**Potées**	Control	2004	0.04	0.02
			2016	-0.11	-0.06
		$Ca/MgCO_3$	2004	0.66	0.34
			2016	0.17	0.08
	Humont	Control	2016	-0.06	-0.02
		$Ca/MgCO_3$	2016	1.35	0.69
	Darney	Control	2016	0.18	0.08
		$CaCO_3$	2016	0.50	0.27

848

849

Electronic Supplementary material

Fig. S1. Description of the methodology to calculated the isotopic composition ($\delta^{26}Mg$) of the 0-15cm soil layer from the measured values of the 0-5 and 5-15 cm soil layers at Potées (1995 and 2004) and Darney (1995) sites.

Fig. S2. Schematic description of the Mg pools and fluxes taken into account in the model. The fluxes with no isotopic fractionation are in black while isotopic fractionating fluxes are in red (alpha values represent the respective isotopic fractionation factor).

Table S3. Description of the different hypotheses tested and results obtained with the numerical modelling approach.

Fig. S4. Relationship between Mg concentration in leaves and $\Delta_{compartments}{}^{26}Mg$. Studied control plots are in blue, studied limed plots in red and literature data in black*.

** (Bedel 2015; Bolou-Bi et al. 2012).*

863 **Fig. S1.**

1) Calculation of the ^{26}Mg and ^{24}Mg ratio for DSM3 (mean on all sessions) :

$$\frac{^{26}Mg}{^{24}Mg}(DSM3) = 0.1592887 \qquad n = 788$$

2) Calculation of the ^{26}Mg and ^{24}Mg ratio for each soil layer sample :

$$\frac{^{26}Mg}{^{24}Mg}(sample) = \left(\left(\frac{\delta^{26}Mg\ (sample)}{1000}\right) + 1\right) \times \frac{^{26}Mg}{^{24}Mg}(DSM3)$$

3) Calculation of the amount of ^{26}Mg for each soil layer sample :

$$\%^{26}Mg\ (sample) = \frac{\frac{^{26}Mg}{^{24}Mg}(sample)}{\left(\left(1 + \frac{^{25}Mg}{^{24}Mg}(DSM3)\right) + \frac{^{26}Mg}{^{24}Mg}(sample)\right)}$$

with $\frac{^{25}Mg}{^{24}Mg}(DSM3) = 0.126742$

4) Calculation of the amount of ^{26}Mg for the 0-15 cm soil layer :

$$\%^{26}Mg\ (0-15cm) = \frac{\left((\%^{26}Mg_{(0-5cm)} \times e_{(0-5cm)} \times [Mg]_{(0-5cm)}) + (\%^{26}Mg_{(5-15cm)} \times e_{(5-15cm)} \times [Mg]_{(5-15cm)})\right)}{\left((e_{(0-5cm)} \times [Mg]_{(0-5cm)}) + (e_{(5-15cm)} \times [Mg]_{(5-15cm)})\right)}$$

with e = thickness of soil layer

[Mg] = Mg concentration of soil layer

5) Calculation of the ^{26}Mg and ^{24}Mg ratio for the 0-15 cm soil layer :

$$\frac{^{26}Mg}{^{24}Mg}(0-15cm) = \frac{\left(\%^{26}Mg_{(0-15cm)} \times \left(1 + \frac{^{25}Mg}{^{24}Mg}(DSM3)\right)\right)}{\left(1 - \%^{26}Mg_{(0-15cm)}\right)}$$

6) Calculation of the $\delta^{26}Mg$ for the 0-15 cm soil layer :

$$\delta^{26}Mg_{(0-15cm)} = \left(\left(\frac{\frac{^{26}Mg}{^{24}Mg}(0-15cm)}{\frac{^{26}Mg}{^{24}Mg}(DSM3)}\right) - 1\right) \times 1000$$

864

865 **Fig. S2.**

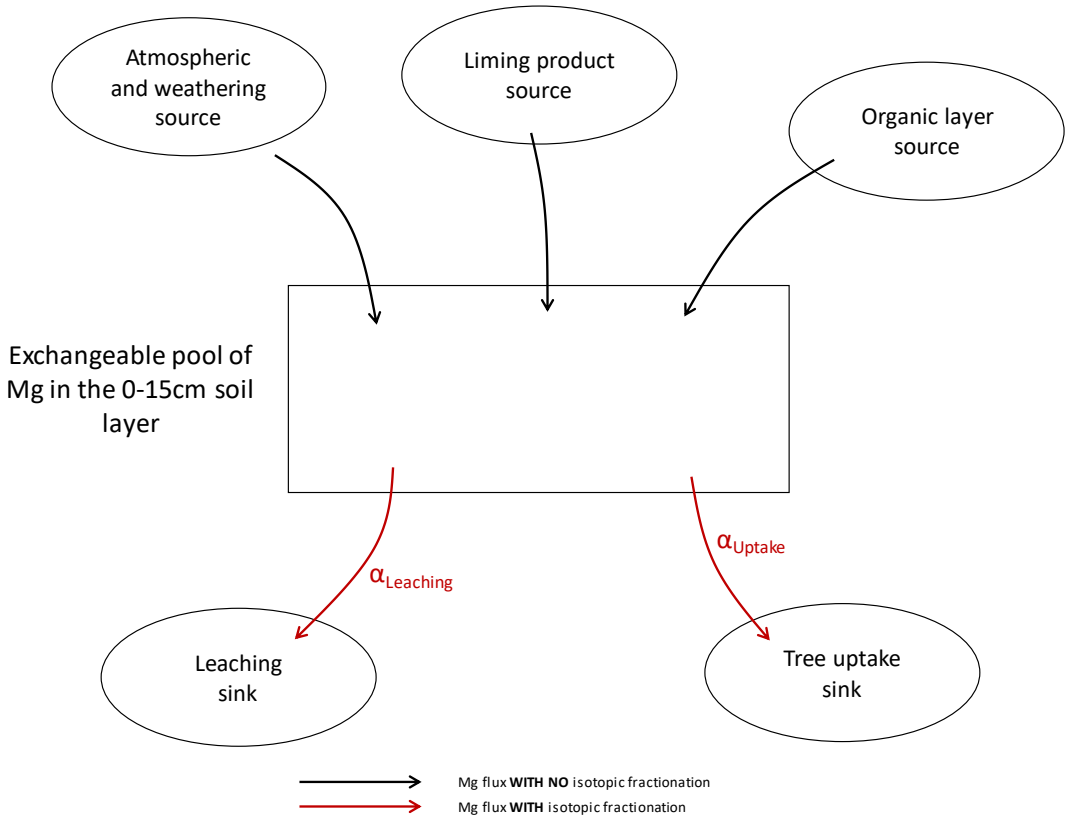

866

Table S3.

Site	Hypothesis	Description/details	Range of input variables tested	Range of simulated parameters	Hypothesis rejected?	Explanation
Darney	The isotopic fractionation during Mg uptake by roots (preferential uptake of 26Mg) explains the differences between limed and control plots	The Mg uptake flux in the limed plot increased after the liming compared to the control (the exchangeable Mg pool was lower in the limed plot) and caused a δ26Mg signature shift in the exchangeable Mg pool.	Mg Uptake: [0.1 : 2.0] $kg.ha^{-1}.yr^{-1}$	α_{Uptake}: [+ 5 : + 10] ‰	YES	The simulated fractionation factors are greater than the Mg isotopic variation at the terrestrial scale and no such fractionation during root adsorption has been reported.
	The isotopic mixing of native exchangeable Mg in the [0-15cm] layer with an input source of Mg with a very low δ26Mg signature explains differences between limed and control plots	The input source of Mg originates from the mineralization of the organic layer after liming. Liming operation have been shown to alter mineralization processes and may have induced the preferential release of 24Mg from the organic layer.	Mg organic layer: 5 $kg.ha^{-1}$ α_{Uptake}: + 0.5 ‰ and +1.0 ‰ Mg Uptake: 0.5 $kg.ha^{-1}.yr^{-1}$ 1.0 $kg.ha^{-1}.yr^{-1}$	δ^{26}Mg organic layer source: [-2.4 : -1.5]‰ [-4.1 : -2.9]‰	YES	The simulated δ^{26}Mg of the organic layer source is much lower than the lowest δ^{26}Mg reported for organic layers (≈-0.5 ‰)
	The input source of Mg originates from the Ca carbonate (reported δ^{26}Mg values for Ca carbonate rocks range from -5‰ to -4‰)		α_{Uptake}: + 0.5 ‰ and +1.0 ‰ Mg Uptake: 0.5 $kg.ha^{-1}.yr^{-1}$ 1.0 $kg.ha^{-1}.yr^{-1}$	Mg input source: [1.9 : 3.0] $kg.ha^{-1}$ [3.3 : 5.2] $kg.ha^{-1}$	NO	To obtain the simulated contributions of a Mg carbonate source the applied carbonate (2500 $kg.ha^{-1}$) would need to contain between 0.13% and 0.34% MgO which is possible
Les Potées	The large fraction of liming product, which was not found in soil (111 $kg.ha^{-1}$), was immobilized in the biomass.		Not modelled		YES	The input-output budgets only show a slight increase of the Mg stock in the biomass in the limed plots (+5 $kg.ha^{-1}$) over the 1995-2004 period.
	The large fraction of liming product, which was not found in soil, was immobilized in the organic layer.		Not modelled		YES	The input-output budgets only shows a slight increase of the Mg stock in the organic layer (+3 $kg.ha^{-1}$) over the 1995-2004 period.
	A large fraction of the Mg released from the liming product was leached below 15cm depth	**A fraction of the liming product was very rapidly (within the 1st year after liming) leached below 15 cm depth and did not isotopically mix with the 0-15cm soil layer**	α_{Uptake}: + 0.5 ‰ and +1.0 ‰ Lime Mg leaching: [0 – 120] $kg.ha^{-1}$	Preferential leaching of dolomitic Mg: [85% : 89%]	NO	The simulated proportion of dolomitic Mg leached below 15cm in only one year agrees with the calculated recovery of dolomitic Mg in 2004 (14 $kg.ha^{-1}$)
		The Mg leaching was associated to an isotopic fractionation	α_{Uptake}: + 0.5 ‰ and +1.0 ‰ Leaching scenarios: - All dolomitic Mg leaching occurs in the first year after application - The leaching of dolomitic Mg is evenly spread over the 10 year period	$\alpha_{Leaching}$: - 0.6 ‰ and -0.4 ‰ - 0.35 ‰ and -0.25 ‰	NO	Though isotopic fractionation during Mg leaching is not well characterized in the literature, the simulated isotopic fractionation factors seem realistic

Fig. S4.

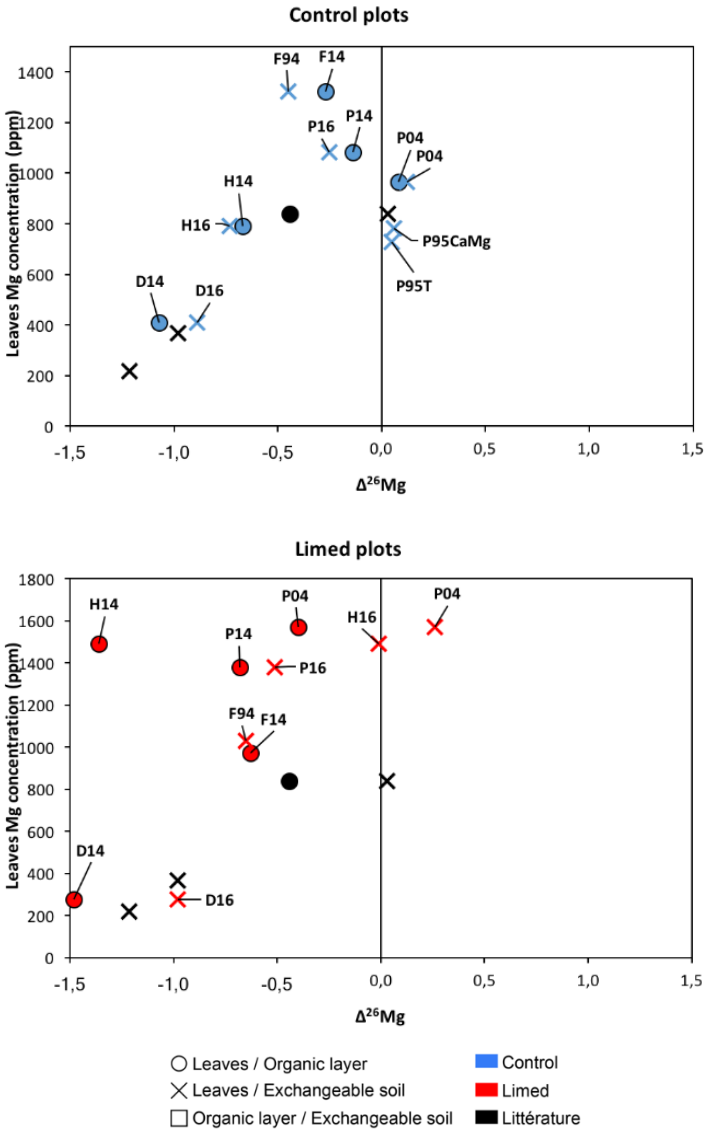
Control plots
Leaves Mg concentration (ppm)
Δ26Mg
F94
F14
P16
P14
P04
P04
H14
H16
P95CaMg
P95T
D14
D16
Limed plots
Leaves Mg concentration (ppm)
Δ26Mg
H14
P04
P04
H16
P14
P16
F94
F14
D14
D16
Leaves / Organic layer
Leaves / Exchangeable soil
Organic layer / Exchangeable soil
Control
Limed
Littérature